



Trabajo Fin de Máster

Estudio de diferenciación y mineralización *in vitro* de osteoblastos en dispositivos microfluídicos

In vitro osteoblasts differentiation and mineralization study inside microfluidic devices

Autor

Pilar Alamán Díez

Directores

Dr. José Manuel García Aznar

D. Gabriele Nasello

ESCUELA DE INGENIERÍA Y ARQUITECTURA
2018



DECLARACIÓN DE AUTORÍA Y ORIGINALIDAD

(Este documento debe acompañar al Trabajo Fin de Grado (TFG)/Trabajo Fin de Máster (TFM) cuando sea depositado para su evaluación).

D./D^a. Pilar Alamán Díez

con nº de DNI 73026321X en aplicación de lo dispuesto en el art.

14 (Derechos de autor) del Acuerdo de 11 de septiembre de 2014, del Consejo de Gobierno, por el que se aprueba el Reglamento de los TFG y TFM de la Universidad de Zaragoza,

Declaro que el presente Trabajo de Fin de (Grado/Máster) Máster, (Título del Trabajo)

Estudio de diferenciación y mineralización in vitro de osteoblastos en dispositivos microfluídicos.

In vitro osteoblasts differentiation and mineralization study inside microfluidic devices

es de mi autoría y es original, no habiéndose utilizado fuente sin ser citada debidamente.

Zaragoza, 19 de noviembre 2018

Fdo: Pilar Alamán Díez

Acknowledgements

En primer lugar quiero agradecer al profesor José Manuel García Aznar, mi director, la oportunidad de poder realizar este trabajo en el grupo de investigación M2BE.

También quiero dar las gracias a Gabriele Nasello y a María Ángeles Pérez por una completa dedicación, supervisión y asesoramiento durante todos estos meses.

Gracias a todos los miembros del grupo M2BE por el compañerismo mostrado durante este tiempo y todo lo que he aprendido de cada uno de ellos.

Por último, agradecer a mi pareja, familia y amigos todo el apoyo que me han mostrado durante la realización de este Máster.

Contents

Acknowledgements	i
List of Figures	iv
List of Tables	vi
Abbreviations	vii
1 Introduction	1
1.1 Clinical issue	1
1.2 Anatomy and physiology	1
1.3 Background	3
1.4 Objective	5
2 Materials and methods	8
2.1 Fabrication of microfluidic devices	8
2.2 Cell culture loading	10
2.2.1 Cell expansion	10
2.2.2 Collagen hydrogel preparation	11
2.2.3 Cell seeded gel loading	13
2.3 Biochemical assays	14
2.3.1 Alkaline phosphatase production	15
2.3.2 DNA assessment	17
2.3.2.1 Hoechst 33258 dyeing protocol	18
2.3.2.2 Microvolumes Plate (TAKE3) DNA quantification	19
2.4 Cell dendrite tracking	20
2.5 Fluorescent staining	20
3 Results	24
3.1 Alkaline phosphatase production tests	24
3.1.1 Collagen hydrogel extraction	24
3.1.2 ALP activity	25
3.1.3 DNA quantification	25
3.1.4 ALP normalization	26
3.2 Cell dendrite tracking	27
3.3 Osteoblasts mineralization and differentiation	29

4 Discussion	32
5 Conclusions	36
A List of chemicals	38
Bibliography	40

List of Figures

1.1	Transitional cell types between preosteoblasts and osteocytes during osteoblast transformation in intramembranous ossification. 1: preosteoblast, 2: preosteoblastic osteoblast, 3: osteoblast, 4: osteoblastic osteocyte (type I preosteocyte), 5: osteoid-osteocyte (type II preosteocyte), 6: type III preosteocyte, 7: young osteocyte, 8: old osteocyte. Adapted from Tamara A. Franz-Odenaal <i>et al</i> 2006.	2
1.2	(a): Microfluidic device where the cells are embedded in collagen hydrogels inside the inner channel. (b): centre channel where cells live (pink color) and reservoir channels where cells receive the culture medium (blue and green channels). Including chemical or biological factors trough one of the reservoir channels triggers a diffusion processes inside due to a chemical gradient inside the hydrogel. Adapted from Oihana Moreno-Arotzarena <i>et al</i> , (2015).	4
1.3	Cellular events in bone remodeling: features of cell types according to their maturation degree. Adapted from Gerald J. Atkins <i>et al.</i> (2011) . . .	5
1.4	Sketch of the inner geometry of the devices. 1: Gel ports. 2: Channel ports. 3: Collagen gel channels. 4: Reservoir/medium channels. 5: Post of the hydrogel channel where hydrogel grips.	6
2.1	Microfluidic devices fabrication process scheme. 1: wafer of the negative inner geometry of the chip made by soft lithography. 2: PDMS mold of the geometry. 3: devices cut individually	8
2.2	3: devices cut into individuals. 4: devices drilled with 4 mm and 1mm biopsy punches.	9
2.3	Hemocytometer used to count cells: 10 μ l of cell suspension was poured between the grid (red square) and a glass surface. Cells in the grid were counted and the final concentrations was calculated by using the formula described above. Picture adapted from supplier website: <i>superior Marienfeld</i>	11
2.4	Color bar for collagen hydrogel pH. Volume of NaOH was adjusted until 7.4 pH was obtained	12
2.5	Prepared hydrogel in a 0.5 ml eppendorf vial containing osteoblasts solution and collagen type I fibers.	12
2.6	Pipetting the hydrogel inside the microfluidic device	13
2.7	Inner geometry of the device with the three central channels full of hydrogel solution containing HOB hydrated with OCM	14
2.8	Schematic sequence of the ALP activity test.	15
2.9	A: dropping DNA solutions in the microplates. B: tool filled and ready to run the measurement. C: spectrophotometer Biotek Synergy HT. . . .	19

3.1	Brightfield microscope picture (magnified at 2X) of the culture chamber of a microfluidic device before and after the extraction of the gel; left and right respectively. After the extraction, there were not remaining cells inside the chamber but just some rests of PBS around the channels. . . .	24
3.2	ALP activity in mU/ml of the HOB at days 3, 7, 14 and 21. Samples were obtained from the 2 hours OCM.	25
3.3	DNA content in ng of the microfluidic devices at days 3, 7, 14 and 21. The samples were obtained out of the extracted hydrogel and measured with the microvolumes plate.	26
3.4	Normalized ALP activity boxplot according DNA content in the samples at days 3, 7, 14 and 21.	27
3.5	Brightfield microscope pictures magnified at 10X of 2D cells and 3D cells (left and right respectively) inside a microfluidic device after 21 days of culture.	28
3.6	Two slides of a brightfield microscope <i>Z-Stack</i> of a mature and dendritic osteoblast, magnified at 20X	28
3.7	Brightfield microscope images of cells connection magnified at 20X	29
3.8	Brightfield microscope pictures magnified at 2X of the culture chamber at days 1 (left) and 21 (right) of culture	29
3.9	Interface of the program developed by Python (<i>ImagePy</i>). The software is able to open pictures and <i>Z-stack</i> in a microscope format and manually select the cell to study	30
3.10	Analyzed cell by the software <i>ImagePy</i> . It is possible to distinguish the cell contour (blue), cell body (red), primary dendrites (yellow) and secondary dendrites (white). The program offers a summary of the cell information (right)	30
3.11	Confocal microscopy picture of a tridimensional osteoblast magnified at 40X. Cell nuclei has been stained with DAPI (blue), calcium deposition of the matrix and cytoplasm is stained by Calcein (green) and BSP2 protein is stained by immunostaining with an <i>AlexaFluor</i> reagent (red)	31
3.12	Confocal microscopy pictures of two tridimensional osteoblasts magnified at 40X. Cell nuclei has been stained with DAPI (blue), calcium deposition of the matrix and cytoplasm is stained by Calcein (green) and DMP1 protein is stained by immunostaining with an <i>AlexaFluor</i> reagent (red) . .	31

List of Tables

2.1	Composition of the collagen hydrogel	12
2.2	Composition of the osteogenic medium	14
2.3	Composition of the standard volume to calibrate the ALP in the spectrophotometry	16
2.4	Composition of standard and sample wells to perform ALP test	16
2.5	Composition of the standard volume to calibrate the DNA content	19
2.6	Composition of standard and sample wells to perform Hoechst DNA assay	19
2.7	Emission and excitation wavelengths of the fluorescence compounds used .	21
A.1	List of chemical reagents, suppliers and catalog numbers	39

Abbreviations

2D	Bidimensional
3D	Tridimensional
ALP	AL kaline P hosphatase
BSP	B one S ialo P rotein
CDU	C ollagen D egradation U nits
DMEM	D ulbecco's M odified E agle M edium
DOC	D ays O f C ulture
DMP	D entin M atrix A cidic P hosphoprotein
EDTA	E thylene D iamine T etracetic A cid
FBS	F etal B ovine S erum
HB	H oechst B uffer
HOB	H uman O steo B lasts
OCM	O steogenic C ulture M edium
PFA	P ara F orm A ldheid
PBS	P hosphate B uffered S aline
PDL	P oly- D - L ysine
PDMS	P olydimetilsiloxan
pNPP	p Nitro P henyl P hosphate
TBS	T ris B uffered S aline

Chapter 1

Introduction

1.1 Clinical issue

Bone remodeling is a dynamic and continuous process required for the maintenance of skeleton architecture which responds to mechanical stimuli [1]. The success of this process means an equilibrium between bone resorption and formation [2, 3]. When the equilibrium breaks, some pathologies arise. Moreover, this imbalance could be also enhanced after the placement of an implant, due to the changes in the mechanical conditions, which ends in aseptic loosening of the implant [4].

The absence of bone matrix production inside scaffolds is one of the main limitation in the field of bone tissue engineering. Bone substitutes do not succeed in replying the unique remodelling capacity of bone tissue yet. Thus, a deeper understanding of the cellular behaviour is clearly necessary for the main types of bone cells [5]. A wider comprehension of the events that occur between cell-environment interaction is crucial to improve natural bone remodeling as well as bone regeneration after placing an implant.

Developing *in vitro* systems that create bone-like tissue has two main purposes that fit here: understanding the mechanisms of bone formation to improve the bone graft outcome and, more in general, replicating *in vivo* conditions to study specific disease or potential therapies [6].

1.2 Anatomy and physiology

The process of bone remodelling is mainly conducted by two cell types: osteoclasts, responsible for bone resorption; and osteoblasts, for bone formation. Osteoclasts are

derived from hemopoietic precursors supplied by the bone marrow, whereas osteoblasts are derived from mesenchymal stem cells in the bone marrow [7–9].

At the end of bone formation phase, osteoblasts can have one of four different fates: become embedded in the bone as osteocytes, transform into inactive osteoblasts, undergo a programmed cell-death (apoptosis) or become cells that deposit chondroid or chondroid bone [10, 11].

Osteocytes are derived from osteoblasts and make up over the 90% of the bone cells [10–13]. However, the mechanism that control the differentiation of osteoblasts into osteocytes embedded in bone matrix is not well understood. Despite that, the regulation of the differentiation process seems to be critical for bone homeostasis [8, 12, 14].

These osteocytes act as mechanosensors that monitor and sense the mechanical environment within bone tissue by signalling to osteoclasts and osteoblasts to remodel. This way, bone strength is maintained throughout life [9, 15, 16].

Osteoblasts-osteocytes transition (figure 1.1) depends on many variables: the mode of ossification (intramembranous, perichondral, endochondral), the type of bone (woven or lamellar bone), the location of bone formation, the species, and on the age and gender of the individual. Franz-Odenaal *et al.* described the effect of each parameter mentioned above [11].

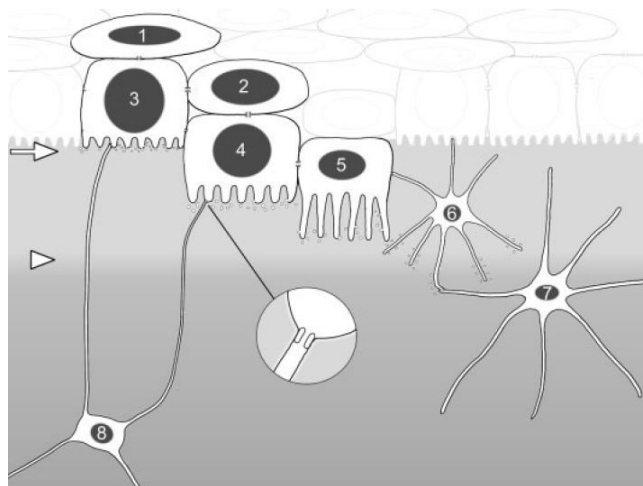


FIGURE 1.1: Transitional cell types between preosteoblasts and osteocytes during osteoblast transformation in intramembranous ossification. 1: preosteoblast, 2: preosteoblastic osteoblast, 3: osteoblast, 4: osteoblastic osteocyte (type I preosteocyte), 5: osteoid-osteocyte (type II preosteocyte), 6: type III preosteocyte, 7: young osteocyte, 8: old osteocyte. Adapted from Tamara A. Franz-Odenaal *et al* 2006.

Osteoblasts morphology is altered from cuboid to dendritic shape during their differentiation to osteocytes [17]. This transition is accompanied by a loss of cell volume,

involving the reduction of organelle content. Moreover, there is an increase in the formation and elongation of projections. The same way, connections with neighbouring osteocytes within the bone extracellular matrix increase, as well as with osteoblasts on the bone surface [13, 18, 19].

Apart from the morphological point of view, gene expression pattern also suffers from a big change: expression of the osteoblasts marker enzyme alkaline phosphatase is reduced, along with a reduction of type I collagen and bone sialoprotein 2 (BSP2), expression of protein E11 is increased and dentin matrix protein 1 (DMP1) is induced with the transformation [9, 20, 21]. Those parameters are detailed below and, some of them, will be used along this work in order to distinguish cellular phenotype.

1.3 Background

In vitro cell mechanobiology studies have proved themselves to be a potential tool to understand bone mechanobiology, which is crucial to the adaptive mechanism of bone. In general, reliable *in vitro* models of bone tissue became a prerequisite tool for a wider comprehension of the biological mechanisms taking place in bone tissue remodeling [22].

One of the most trending technique adapted from the past years to perform *in vitro* studies is microfluidics. The microfluidics is a technique that allows to work with volumes in small scale, typically submillimetric, where capillarity domains the mass transportation [23, 24]. This reduction in dimensions involves saving chemical reagents, space and wastes. Moreover, working in micro-scale systems allow greater control and versatility in therms of pH and temperature [25].

Microfluidic-based devices are a good approach to evaluate the regulatory effects of single mechano-chemical cues on cell behaviour. They also showed a flair for reproducing bone tissue-like models by combining multiple stimuli and, hence, creating more *in vivo*-like environment [26]. Furthermore, microfluidic platforms allow long-term culture of bone cells over the 3D environment (essential for bone tissue culture) with a limited number of cells and reagents per sample [13, 27].

Microfluidic devices allow to recreate physiological cellular microenvironments by including biomimetic hydrogels and generating controlled chemical gradients. Here, hydrogels made of collagen were selected because it is the major protein component of nature bone, and it is the precursors matrix for direct bone repair [28]. This gels also favour isolate factors for study, simulate laboratory analysis and modeling cellular, tissue and organ level processes [22]. See in the figure 1.2 a picture of a simple microfluidic device

which allows to put the cells through a chemical gradient in order to study the effects of a growth factor [25].

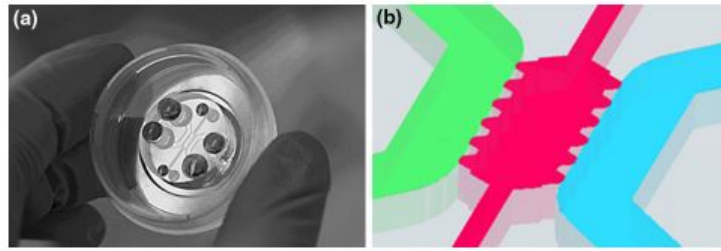


FIGURE 1.2: (a): Microfluidic device where the cells are embedded in collagen hydrogels inside the inner channel. (b): centre channel where cells live (pink color) and reservoir channels where cells receive the culture medium (blue and green channels). Including chemical or biological factors through one of the reservoir channels triggers a diffusion process inside due to a chemical gradient inside the hydrogel. Adapted from Oihana Moreno-Arotzarena *et al.*, (2015).

As mentioned above, collagen hydrogels are widely used for *in vitro* experiments and tissue engineering applications, becoming one of the best alternatives to substitute biological tissue in cell culture. Those hydrogels consist in a polymer network made of connected filaments embedded on an aqueous medium [29, 30]. The final stiffness of the hydrogel depends on both individual and global structure properties [31].

Dense fibrillar collagen matrices have been developed with the aim of replicating the composition and the structure of actual osteoid tissue. Thanks to the composition, texture and density, these matrices were proposed as connective tissue model for cell culture [32]. The collagen hydrogel matrices provide an appropriate three dimensional microenvironment for the adhesion, migration, proliferation and differentiation of osteoblast. Type I collagen is the major component of bone matrix and is widely used in cell culture because is well known to induce the differentiation of mesenchymal cell types [15, 33]. Summing up, cell cultured in type I collagen gels maintain their function and ensure a 3D structure and the cell-cell interaction [14, 29, 34].

Researchers already cultured osteoblasts in type I collagen gel and they added supplements to enhance the osteogenic behaviour: β -Glycerol phosphate and ascorbic acid [12, 14, 35]. Here, a tridimensional culture is done by combining microfluidic devices and collagen hydrogel. These 3D culture systems enhance osteoblastic and osteocytic gene expression compared with cells cultured in 2D monolayer [12].

Some chemical assays are widely used in these *in vitro* experiments to discriminate cell phenotype. As commented above, some biomolecules have been selected from the literature as markers in osteogenic differentiation for this work [10, 11, 20, 36–39]. See a resume of each cell type characteristics in figure 1.3:

- Alkaline phosphatase (ALP): it is an enzyme that induces dephosphorylation of organic compounds. ALP is produced by osteoblasts and it is released in cell culture medium in the early stages of bone formation. ALP is widely recognized as osteogenic marker for osteoblasts, whose concentration gets maximum values at the beginning of the cell life and later, decreases when mineralization takes place [39–41].
- Bone sialoprotein II (BSP2): it is present in bone and other mineralized tissues. Bone cells produce this protein in early osteoblast differentiation stages. By monitoring this protein, it is possible to study cell expression of mature osteoblast phenotype [39].
- Dentin matrix production (DMP1): it is an extracellular matrix protein, critical for proper mineralization of bone. In undifferentiated osteoblasts it is primarily a nuclear protein that regulates the expression of osteoblast-specific genes. During osteoblast maturation the protein becomes phosphorylated and is exported to the extracellular matrix, where it orchestrates mineralized matrix formation [42]. By monitoring this protein in the matrix, osteoblasts differentiation to osteocytes can be studied.

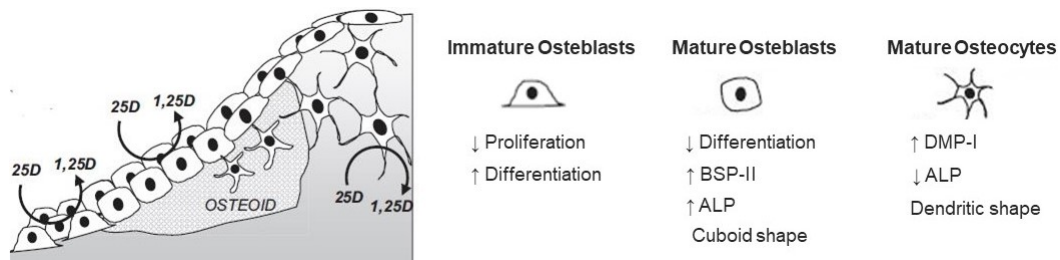


FIGURE 1.3: Cellular events in bone remodeling: features of cell types according to their maturation degree. Adapted from Gerald J. Atkins *et al.* (2011)

1.4 Objective

The final goal of this work was to perform an *in vitro* bone model inside microfluidic devices in order to study osteoblasts behaviour. The different tasks aimed to study osteogenic differentiation and bone matrix production of osteoblasts. The cell markers previously commented were quantified and cell connections and interactions were tracked.

Understanding the regulatory mechanisms of osteoblast-osteocyte differentiation are of significant for the development of bone forming reagents for the treatment of some pathologies as osteoporosis, tissue engineering for regenerative medicine or to improve

the osteointegration of prostheses. The obtained results might help to understand which stimuli further improve bone regeneration and remodeling to apply, for instance, some physical or biochemical conditions within the placement of a prosthesis.

Human osteoblasts (HOB) were seeded inside microfluidic devices and fed with Osteogenic Culture Medium (OCM) containing the supplements recommended in bibliography [12]. HOB progressive differentiation and mineralization was followed by performing different experiments along several timepoints.

Notice that the device shown in the figure 1.2 (b), has micropillars in the centre channel which enclose the area. These posts retain the gel solution by hydrophobic surface tension. In this work, similar microfluidic devices were used. However, the chamber was composed of three channels instead of one. This difference is owing to the strength that primary osteoblasts are able to do. If providing the collagen matrix with three channels, the hydrogel finds more posts to bind to, so it is more difficult to detach. See in the picture 1.4 a scheme of the geometry used.

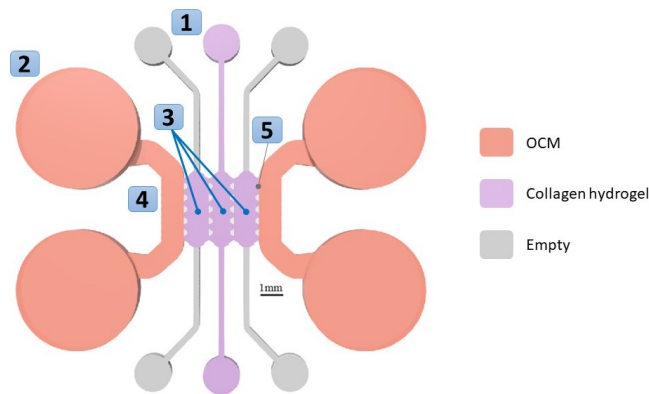


FIGURE 1.4: Sketch of the inner geometry of the devices. 1: Gel ports. 2: Channel ports. 3: Collagen gel channels. 4: Reservoir/medium channels. 5: Post of the hydrogel channel where hydrogel grips.

Additionally to the three cell channels (figure 1.4-3), two media channels are in direct contact to them (figure 1.4-4), through which OCM was provided to the cells. The culture was incubated at 37°C in a $5\% \text{CO}_2$ atmosphere with replacement of medium every 2-3 days.

In order to discriminate osteoblasts-osteocytes cell type, several markers from the literature were selected: the enzyme ALP, Calcium deposition and proteins BSP2 and DMP1 [11]. In this work, DMP1 and BSP2 released in the matrix was assessed by immunofluorescent staining, while biochemical assays were performed to determine cell number and ALP activity. Moreover, the expression of cell dendrites, which are characteristic of osteocytes phenotype, were tracked by brightfield microscopy.

The experimental tasks were developed in a professional laboratory belonging to the research group Multiscale in Mechanical and Biological Engineering (M2BE) inside Aragón Institute of Engineering Research (I3A) at the University of Zaragoza. This project is framed and funded within an European project Curabone (number 722535) whose global aim is to integrate numerical simulation technologies based on image analysis in order to enhance the customized treatments to bone fractures healing and its long term evolution.

Chapter 2

Materials and methods

2.1 Fabrication of microfluidic devices

Microfluidic devices with three culture channels were fabricated following a protocol adapted from C. Del Amo *et al.* (Integrative Biology, 9: 339-349, 2017) [43]. They are made of polydimethylsiloxane (PDMS) due to its physicochemical properties.

The total procedure to manufacture each batch of devices takes 5 days. Several bunches of devices were done in this work following the protocol explained in the following paragraphs (summarized in figures 2.1 and 2.2).

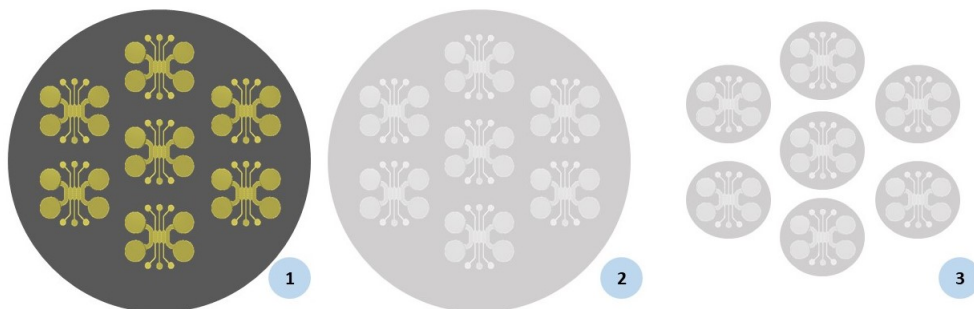


FIGURE 2.1: Microfluidic devices fabrication process scheme. 1: wafer of the negative inner geometry of the chip made by soft lithography. 2: PDMS mold of the geometry. 3: devices cut individually

Day 1 - The first day, a mold of the desired inner geometry was done. To fabricate the mold, a wafer with the required inner geometry was needed. Those masters were externally purchased and manufactured by lithography (figure 2.1-1).

Liquid PDMS solution was prepared by mixing Sylgard 184 silicone elastomer base (VWR) and the curing agent in a 10:1 weight ratio (30 g silicone + 3 g curing agent per wafer). After mixing the solution using a spatula, it was needed to degas it to remove

air bubbles. Then, liquid silicone was poured in the wafer of the geometry and degassed again. The last step was to cure the solution in an oven at 80°C overnight.

Day 2 - The next day, the solidified silicone was taken out of the oven and detached from the wafer by using a scalpel (figure 2.1-2). Then, the seven geometries were punched with a 20 mm circular blade (figure 2.2-3) and the holes for the cells and media channels were drilled by using disposable biopsy punches, 1 mm and 4 mm diameter respectively (figure 2.2-4). After that, the devices had to be sterilized in two steps of autoclave. Then, they were placed in an oven at 80°C overnight.

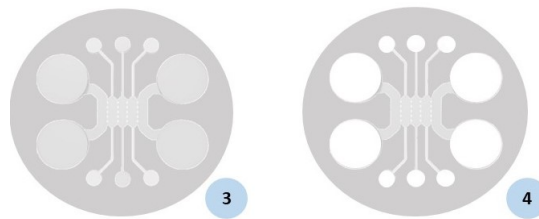


FIGURE 2.2: 3: devices cut into individuals. 4: devices drilled with 4 mm and 1mm biopsy punches.

Day 3 - The silicone devices were sealed to their glass covers (Ibidi Glass Bottom μ -Dish 35 mm). The covers grant a glass base to the 3D culture and make cell culture visible under microscope. Moreover, they are shrouded, providing protection and sterility. With this purpose, the devices and glass covers were placed in a plasma cleaner, geometry side up. Glass covers lids were saved in a Petri dish where they are sterilized later by UV light.

The vacuum pump and the plasma chamber were turned on to treat the surfaces of PDMS and glass covers for two minutes. After this time, each device was bonded and softly pressed to its glass coverslip. Now, inside a laminar flow hood, channels were filled with 60 μ l of surface coating solution Poly-D-lysine (PDL) and devices were placed in an incubator for four hours. PDL is a synthetic molecule that improves cellular adhesion and proteins absorption by changing superficial charges of the hydrogel. Besides, this treatment ease the union between PDMS and the hydrogel surface.

Afterwards, PDL solution in the channels was thoroughly removed by vacuuming. Since an excess of PDL can cause cell damage, the chamber was filled with 300 μ l of sterile deionized water using a micropipette in order to wash them. This procedure was repeated until devices were filled with DI water from all inlets: filling and taking water out from the opposite inlets. Then, all microfluidic channels were completely aspirated. Finally, coated devices were placed in a sterile dish at 80°C for 48 hours.

Day 5 - Samples were taken out of the 80°C oven. When they reach room temperature, they can be either used or stored at up to one month.

2.2 Cell culture loading

2.2.1 Cell expansion

Primary Human Osteoblasts (HOB, PromoCell) were cultured at 60% to 75% confluence. These cells were isolated from donated human tissue at passage 1. As HOB growth mode is adherent, cells were cultured and expanded in 2D inside culture flasks (T-25, 25-cm², 7ml) forming a monolayer all over the inner surface in Dubelco's Modified Eagle Medium (DMEM, Gibco). DMEM expansion medium contains 10% heat-inactivated fetal bovine serum (FBS, Lonza), 100 U/mL penicillin, and 100 µg/mL streptomycin (Lonza). Cultures were incubated at 37°C in a 5% CO₂ atmosphere with replacement of medium every 2-3 days.

It was necessary to take cells out of the flask in order to prepare the cell solution. The first step was to trypsinize the cells in order to detach them from the surface. With this purpose, old medium in the flask was removed with a Pasteur pipette (carefully from the opposite corner of the flask neck). Then, 3 ml of Phosphate Buffered Saline (PBS) were poured inside the flask to wash the cells to remove residual FBS that could inactivate the trypsin. This step was repeated twice.

After that, 500 µl of trypsin (TrypLETM Express Enzyme, Invitrogen) were poured inside the flask. Then, it was rapidly put inside the incubator at 37°C for 1 minute. After 1 minute, 1 ml of DMEM was added. Cell suspension (+ 500 µl of trypsin + 1 ml of DMEM) was drawn into a tip of a P-1000 pipette and the whole solution was rinsed two or three times to dissociate cells and to dislodge any remaining adherent cells. Then, cell suspension was passed to a sterile 15 ml centrifuge tube.

10 µl of the cell suspension were taken to count cell concentration by using a hemacytometer. In the same tube, the suspension was centrifuged for 5 minutes at 1500 rpm. The subsequent supernatant was removed and fresh DMEM was added, so all the remainder trypsin was removed. The volume of resuspension medium depends on the number of cells counted previously and the final cell concentration in the gel desired for the experiment.

The determination of the number of cells in culture is important for standardizing culture conditions and performing accurate quantification experiments. Thus, the 10 µl taken from the previous solution were placed in the Neubauer chamber (hemocytometer, figure 2.3). It is a microscopic counting grid that was used to determine the density of a cell suspension. This tool enable to estimate the percentage of viable cells in the whole population. It was needed to use that chamber when performing the collagen hydrogel

in order to set the cell concentration inside the device. Once the Neubauer chamber was loaded, it was placed on the microscope and a hand-held counter was used to count cells.

$$\frac{\text{cells}}{\text{ml}} = \text{average count per square} \times 10^4$$

$$\text{total cells} = \frac{\text{cells}}{\text{ml}} \times \begin{array}{l} \text{total original volume of cell suspension} \\ \text{from which sample was taken} \end{array}$$

The volume correction factor for the tool is 10^4 : each square is $1 \times 1 \text{ mm}$ and the depth is 0.1 mm .

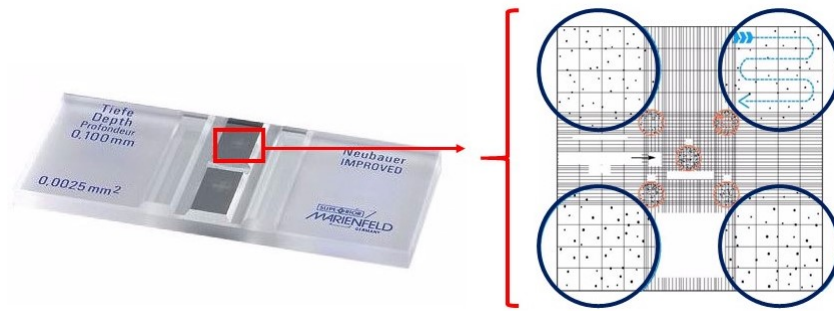


FIGURE 2.3: Hemacytometer used to count cells: $10 \mu\text{l}$ of cell suspension was poured between the grid (red square) and a glass surface. Cells in the grid were counted and the final concentrations was calculated by using the formula described above. Picture adapted from supplier website: *superior Marienfeld*.

Cell solution after centrifugation should be five times higher than the final concentration desired in the device because it is diluted five times during the seeded hydrogel preparation (table 2.1).

2.2.2 Collagen hydrogel preparation

A high density collagen hydrogel was prepared. The collagen final concentration was 6 mg/ml . $200 \mu\text{l}$ of gel were enough to seed up to 17 three-channel devices (figure 1.4).

Since collagen is normally stored in highly acidic solution, the gel pH must be adjusted before adding the cell suspension. The pH of the gel was brought to 7.4 for culturing HOB. Chemicals used to make the collagen seeded hydrogel solution are listed below:

- Collagen I, Rat Tail 8.90 mg/ml (Corning).
- 10X phosphate buffered saline (DPBS) with phenol red (Euroclone).

- 0.5 M NaOH solution: 5 g of NaOH tablets (Sigma-Aldrich) were dissolved in 230 ml of sterile deionized water by stirring. Then, this solution was sterilized using a 0.2 μm filter and, finally, the it can be stored at room temperature.
- Cell solution: during the collagen hydrogel preparation, a fixed volume of cell solution was added independently from the final cell concentration required. This was done to minimize errors in the loading phase due to pipetting. Table 2 shows the volumes of the chemicals used to make 200 μl of gel.

Compound	%	Volume for 200 μl gel
Collagen	67,3%	134,84 μl
NaOH 0,5 M	2,7%	5,4 μl
10x DPBS	10%	20 μl
Cell solution	20%	40 μl

TABLE 2.1: Composition of the collagen hydrogel

Remark: *those quantities were set for accurate 7.4 pH in a 200 μl gel. If necessary, they could be modified in order to get 100 μl or 300 μl . However, the volume of NaOH solution that achieves pH 7,4 does not follow a linear relation, it needs to be readjusted. Figure 2.4 shows the color bar used to rapidly identify the pH of the gel.*

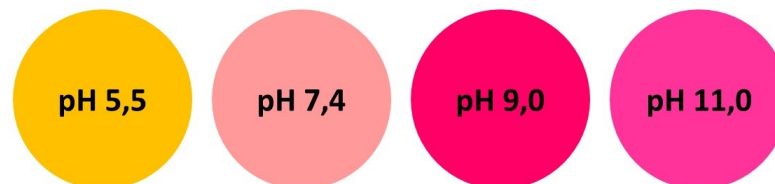
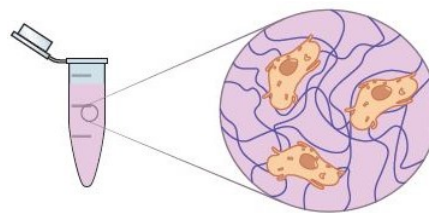


FIGURE 2.4: Color bar for collagen hydrogel pH. Volume of NaOH was adjusted until 7.4 pH was obtained



Collagen Seeded Hydrogel

FIGURE 2.5: Prepared hydrogel in a 0.5 ml eppendorf vial containing osteoblasts solution and collagen type I fibers.

2.2.3 Cell seeded gel loading

The first step was to place every compound inside a ice bucket in order to avoid early collagen polymerization. Then, the quantities of the compounds indicated in the table 2.1 were added and gently mixed with a pipette inside a cold vial. When taking the collagen from the aliquot it is necessary to do it slowly, waiting when the pipette gets its limit and retract it. Then, the collagen pouring has to be gentle as well.

The procedure of preparing the collagen hydrogel and seed it into the devices must not take more than one hour (final result in figure 2.5). The gel used during this project had a collagen concentration of 6 mg/ml, but this value can be adapted to prepare hydrogels with different concentrations by diluting the base solution before polymerization. Cell final concentration used during these experiments was set to 250.000 cells/ml.

The collagen gel solution was slowly filled into the microfluidic devices through the middle port (figure 1.4, number 1) as it is shown in the figure 2.6. It is recommended to fill three devices at a time with 20 μ l of gel suspension.



FIGURE 2.6: Pipetting the hydrogel inside the microfluidic device

To initiate polymerization, the gel-filled devices were quickly placed in the prepared humid chamber with the channel side facing down. As the collagen gel polymerization is thermally induced by heating the gel solution, the humid chamber was put in a CO_2 incubator at 37°C for 2.5 minutes.

After this time, the humid chamber was moved under the hood and the devices were placed channel-upside. The humid chamber was placed again in a CO_2 incubator for 5 minutes. this procedure was repeated 2 times (upside - downside) and, finally, the channel side was moved face down for 2.5 minutes. The overall polymerization process takes 20 minutes.

Remark: *after the seeding inside the devices, cells will be fed with Osteogenic Culture Medium (OCM) to induce osteogenesis. OCM is composed*

of the expansion medium supplemented with 50 $\mu\text{g}/\text{mL}$ ascorbic acid, 10 mM β Glycerol-phosphate. The table 2.2 shows the final composition of the OCM:

Compound	Composition
DMEM	$\approx 89\%$
FBS	10%
Antibiotics	1%
L-Glutamine	2 mM
β Glycerol phosphatase	10 mM (1%)
Ascorbic acid	50 μM (0.03%)

TABLE 2.2: Composition of the osteogenic medium

Once polymerization was completed, OCM was added in all reservoirs of the device. OCM was gently added through one reservoir well until the medium was observed in the connected one. After that, all reservoirs were completely filled (200 μl each device). The lids (sterilized by UV light) were placed covering the devices. Once hydrated with OCM, devices were kept within a Petri dish in the incubator (37°C and 5% CO₂). The final result of the seeding is shown in the figure 2.7.

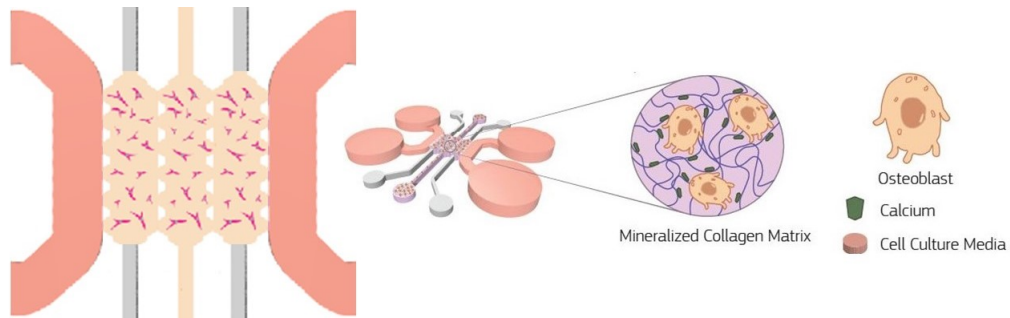


FIGURE 2.7: Inner geometry of the device with the three central channels full of hydrogel solution containing HOB hydrated with OCM

Remark: *it is needed to exchange the medium every 2 - 3 days. In order to do that, the old medium was gently vacuumed through the medium channels (figure 1.4-2). Then, the same volume of fresh medium per device (200 μl) was added with a pipette in one channel by dropping, letting the medium enter into it. Inside the chamber, fresh nutrients reach the cells by diffusion through the gel.*

2.3 Biochemical assays

Two different biochemical tests were performed: Alkaline Phosphatase (ALP) production test and DNA quantification assessment. Each timepoint of the experiment, three

devices were studied.

2.3.1 Alkaline phosphatase production

ALP activity was determined using a colorimetric assay of enzyme activity (SIGMAFAST p-NPP Kit, Sigma Aldrich), which uses p-nitrophenyl phosphate (pNPP) as a phosphatase substrate, with ALP enzyme from bovine intestinal mucosa (Sigma Aldrich) as a standard. The substrate changes its absorbance wavelength when dephosphorylated by ALP. The change in emission is measured at 540 nm on a plate reader (Biotek synergy HT). Results were then normalized to cell number and the final results were expressed in units of ALP per nanogram of genetic material.

ALP samples were taken at every timepoint of the experiment out of the culture medium of the devices. Firstly, the devices were taken out from the incubator and, inside a laminar flow hood, old culture medium was removed. Then, 200 μl of fresh medium per device were poured and afterwards, devices were placed in a incubator for, exactly, two hours. After this time, the new medium was isolated and stored in vials. This vials are stored at -20°C and they were the actual samples obtained from the devices. In this way, the same volume per device (200 μl) incubated the same time was obtained, avoiding ALP denaturation that occurs in old medium.

ALP activity was measured by absorbance (protocol modified from the original proposed by Birmingham *et al.* in 2012) [33]. Figure 2.8 shows a summary of the total procedure followed, which is detailed in the following paragraphs.

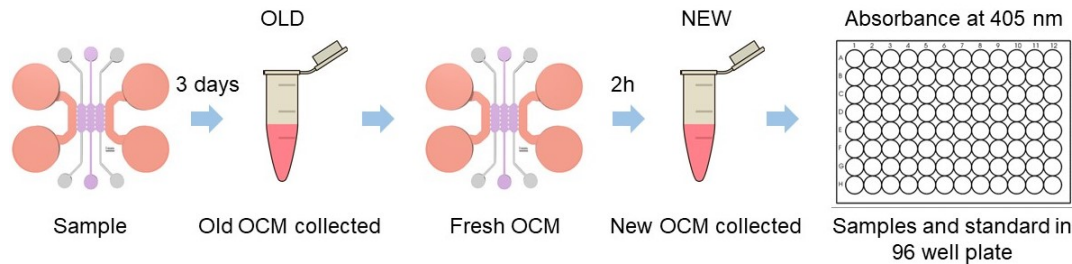


FIGURE 2.8: Schematic sequence of the ALP activity test.

In order to measure the ALP production of the cells depending on the day of culture, a spectrophotometry of the collected culture medium was done. To test the enzymatic production, these samples were compared with standard quantities containing a fixed and known quantity of the enzyme. The standard wells were determined by using known amounts of Alkaline phosphatase from bovine intestinal mucosa (Sigma-Aldrich). Find, in the table 2.3, the volumes to make the control standard solutions.

Standard	pNPP (μl)	ddH ₂ O (μl)	OCM (μl)	Final pNPP (nmol/ μl)
Blank/C0	0	320	160	0
C1	4	316	160	0.03
C2	8	312	160	0.07
C3	16	304	160	0.10
C4	32	288	160	0.13
C5	48	272	160	0.17
C6	64	256	160	0.33
C7	80	240	160	0.67

TABLE 2.3: Composition of the standard volume to calibrate the ALP in the spectrophotometry

A 96-well plate was filled with the different samples that were stored with fixed quantities of ALP as control. 40 μl of collected medium were added to the 96-well plate in triplicates with 50 μl of pNPP solution, which contained both pNPP and assay buffer (PBS).

The standard wells were filled with 120 μl of the corresponding standard volume and 10 μl of ALP enzyme. Sample wells were filled with 50 μl of the 5 mM pNPP solution, 40 μl of the sample (obtained out of the culture medium stored) and 40 μl of deionized water. All wells had a final volume of 130 μl (see a summary in table 2.4).

Standard well	Sample Well
120 μl standard solution	50 μl 5mM pNPP solution
10 μl ALP enzyme	40 μl sample
-	40 μl deionized water
130 μl total	130 μl total

TABLE 2.4: Composition of standard and sample wells to perform ALP test

Then, the well plate was left 1 hour to allow the substrate and the enzyme to bind. After one hour, the plate was placed in the spectrometer and the absorbance measurement was performed at 405 nm in a Synergy HT Multimode microplate reader.

Solutions for ALP assay: two solutions were prepared to perform the assay described above:

- 5 mM pNPP solution: one tablet of pNPP and one tablet of TRIS buffer were diluted in 5 ml of deionized water (Sigma-Aldrich Kit).
- ALP enzyme solution: 1 μl of ALP enzyme (commercial 43kU/ml) was diluted in 10 ml of deionized water.

2.3.2 DNA assessment

To quantify the DNA amount it was needed to extract the cells out of the devices. A collagenase solution was required to degrade the collagen matrix and isolate the embedded cell. The collagenase enzymatic activity was measured in collagen degradation units per ml (CDU/ml). One CDU per ml liberates peptides from collagen equivalent in ninhydrin color to 1.0 mmole of L-leucine in 5 hours at pH 7.4 at 37°C in the presence of calcium ions [44].

Regarding the results obtained in literature, the goal solution had an activity of 514 CDU/ml [45]. This solution was prepared diluting 30 mg of collagenase powder (Sigma-Aldrich, 257 units/mg) in 15 ml of PBS. Thus, the collagenase solution final concentration was 2 mg/ml obtaining 514 CDU. 15 ml of total volume were prepared and separated in 650 μ l aliquots.

After the medium collection for ALP samples, the devices were washed twice with PBS for 5 minutes. Then, 200 μ l of the collagenase solution were poured in each device (100 μ l each two medium holes). Finally, devices containing collagenase solution were kept at 37°C on a shaker overnight while the collagen degradation was taking place.

The next day, the devices were taken out of the incubator. Inside a laminar flow hood, the gel was gently extracted with a pipette through the middle gel channel hole. Then, the extracted gel was poured in a vial (one vial per device). As there were remaining cells in the bottom of the device, 200 μ l of PBS were poured in the chamber and it was washed by pipetting twice. In order to isolate all residual cells, the PBS used to wash was also collected in the cell vials.

In order to remove the collagenase, vials (containing cells + collagenase + PBS used for washing) were centrifuged for 5 minutes at 1500 g. Afterwards, the supernatant was removed with a pipette and kept in other vial (wastes vial). Then, cells were resuspended in 500 μ l of PBS and centrifuged again. Finally, the supernatant was taken and kept in the wastes vial. Cells vials were stored at -80°C and wastes vials at -20°C.

DNA amount at each timepoint was measured with two different procedures. The first one follows a widely accepted method based on a fluorescence assay: Hoechst 33258 dye. The second method uses a specific tool to measure DNA directly in a special microplate: a complement device of Biotek Synergy spectrophotometer.

2.3.2.1 Hoechst 33258 dyeing protocol

Solutions for Hoechst procedure: several solutions were done to perform the assay described below:

- Hoechst dye solution: 1mg/ml Hoechst dye in deionized water. This solution is directly provided by the supplier (Sigma-Aldrich) in the right concentration.
- 10x Hoechst buffer (HB): 6.05 g TRIZMA base (Sigma-Aldrich), 1.85 g EDTA (Sigma-Aldrich), 29.20 g NaCl (Sigma-Aldrich) in 500 ml of deionized water. After preparing the solution, the pH was adjusted to 7,4 using concentrated HCl, NaOH and a pH meter.
- Working dye solution: 2 ml 10xHB and 2 μ l Hoechst dye solution were diluted in 18 ml deionized water.
- DNA standard: commercial DNA salt (Sigma-Aldrich) was dissolved in 10xHB at 1mg/ml. Then, it was diluted 50 times in sterile deionized water (to 20 μ g/ml).

An adapted protocol for Hoechst 33258 widely used was followed [46]. This technique consist on dying DNA with the Hoechst solution and quantify it by fluorescence. The quantification was done by comparing the fluorescence obtained with results from standards; which were made of Deoxyribonucleic acid sodium salt from calf thymus.

The procedure began by thawing the frozen samples of isolated cells. Then, 250 μ l of a tampon solution of 10XHB per sample (detailed above). This buffer stabilizes the DNA, so the whole test was performed using this buffer as solvent.

After that, the sample must undergo to at least 2 freezing and thawing cycles. This procedure induces breakage of cell membranes and DNA release in the solution. Samples may be stored temporarily at the third thaw. However, it is better to thaw the samples and carry out the Hoechst assay while transferring the remaining sample to 0.5-1 ml tubes for storage at -80°C .

In order to quantify the amount of DNA in the samples, standards were prepared. See table 2.5 the volume used for this preparation.

Afterwards, the working dye solution was prepared in minimal light conditions (composition detailed above). Once this solution was prepared, 20 μ l of each standard/ sample saolution were added into individual wells (triplicates). Finally, in minimal light conditions, 200 μ l of the working dye solution were added to each well using multi-channel pipette. Table 2.6 shows the composition of both sample and standard wells.

Standard	DNA/well [ng]	4X scale mix	DNA standard (μl)	1XHB 80 μl
Blank/C0	0	0	0	80
C1	15	60	3	77
C2	30	120	6	74
C3	45	180	9	71
C4	75	300	15	65
C5	150	600	30	50
C6	225	900	45	35
C7	300	1200	60	20

TABLE 2.5: Composition of the standard volume to calibrate the DNA content

Standard well	Sample Well
20 μl standard solution	20 μl sample solution
200 μl working dye solution	200 μl working dye solution
220 μl total	220 μl total

TABLE 2.6: Composition of standard and sample wells to perform Hoechst DNA assay

The plate was placed in the spectrophotometer on fluorescence mode and emission and excitation were measured at 485 nm and 380 nm respectively.

2.3.2.2 Microvolumes Plate (TAKE3) DNA quantification

The second technique used to quantify DNA content in the microfluidic devices was: Multi-Volume Analysis of Nucleic Acids Using the EpochTM Spectrophotometer System (Biotek, Synergy HT). This tool allows to measure nanograms of DNA per μl in a single 3 μl drop of the sample solution. See in the figure 2.9, a picture of the DNA reader tool and the spectrophotometer.



FIGURE 2.9: A: dropping DNA solutions in the microplates. B: tool filled and ready to run the measurement. C: spectrophotometer Biotek Synergy HT.

Having the samples frozen at -80°C , it was needed to do the freezing-thawing cycles to lyse the membrane the same way as explained in the Hoechst procedure.

Previous to the placement of the samples in the the microvolume plate, it was washed with PBS and ethanol 70%. Then, 3 μ l of PBS were dropped in each micro well to make a first measure as a blank control.

Afterwards, 3 μ l of each sample were taken and dropped in the plate as shown in the figure 2.9 (A). Finally, the TAKE3 program of the spectrophotometer software was used to read DNA content.

DNA content measure consists of a direct quantification of nucleic acids using the spectrophotometric absorbance at 260 nm. This fact is possible due to the subnanometric structure composition of genetic material [47].

2.4 Cell dendrite tracking

Brightfield microscope (Nikon D-Eclipse C1 Confocal Microscope) was used to track cell dendrites in real-time, while cell culture is taking place. In order to track cell dendrites, several pictures in *Z-Stack* mode were taken to watch cells in 3D. The *Z-Stack* consists in taking pictures of a region increasing the step through a sample. Brightfield microscopy was done every 4 - 5 days during the entire duration of the experimentation phase.

As a future task inside this project, a tracking software will be developed where, analyzing the *Z-Stack* pictures, the user will be able to extract: the geometry of the cell dendrites, the number of dendrites and the connections between them.

2.5 Fluorescent staining

Cell morphology, Calcium deposition and proteins release were determined by confocal microscopy. The microscope used was Zeis LSM880 confocal microscope.

Several stains were used to dye the samples in order to differentiate the components of the cell and specific proteins inside the cytoplasm as well as compounds released in the matrix (table 2.7):

- DAPI (Invitrogen): it is a fluorescence stain that binds strongly to DNA so it allows the user to watch the cell nuclei in a fluorescence microscope. The excitation and emission wavelengths are 340 and 454 nm respectively.
- Phalloidin TRIC, Tetramethylrhodamine B isothiocyanate, (Sigma-Aldrich): it is a fluorescence stain that binds actin filaments so that makes it possible to observe

part of the cytoskeleton as well as distinguish cell contour. The excitation and emission wavelengths are 540 and 570 nm respectively.

- Calcein (Sigma-Aldrich): it is a non toxic fluorescence stain that binds the Calcium so it allows the user to watch the calcium deposition in the extracellular matrix. The excitation and emission wavelengths are 470 and 509 nm respectively.

Apart from those, which are used to perform a regular staining, two primary antibodies and two fluorescent secondary antibodies were used to make an immunostaining. This approach consists of using a couple of antibodies to bind targeted biomolecules. Firstly, the primary one binds selectively to the target. Then, the secondary antibody, which is the fluorescent one acting like a label, binds to the primary. When exciting the sample with excitation wavelength of the secondary antibody, its emission is detected if the sample contains the targeted biomolecule.

The antibodies used are provided by Santa Cruz Biotechnology supplier:

- Primary antibody:
 - Mouse monoclonal Anti-BSP2. As commented in Chapter 1, BSP2 is a protein typical in cell expression of mature osteoblasts phenotype.
 - Mouse monoclonal Anti-DMP1. As commented in Chapter 1, DMP1 is a protein that indicates the osteoblasts-osteocytes transition.
- Secondary antibody (*Alexa fluor* compounds):
 - Mouse IgGKappa secondary CruzFluor 594 (table 2.7).
 - Mouse IgGKappa secondary CruzFluor 680 (table 2.7).

Compound	Emission	Excitation
DAPI	454-488 nm	340-364 nm
Phalloidin	570-573 nm	540-545 nm
Calcein	509 nm	470 nm
IgG 594	614 nm	594 nm
IgG 680	701 nm	680 nm

TABLE 2.7: Emission and excitation wavelengths of the fluorescence compounds used

DAPI, Phalloidin and antibodies solutions were supplied directly in the appropriate stain concentration. However, Calcein was bought in powder, so it needed to be diluted before use.

To prepare the Calcein solution at the concentration of 2.5 mg/ml (the one used in bibliography [30]), 5 mg of Calcein powder were dissolved in 2 ml 0.5 M NaOH solution. After homogenizing, the solution was sterilized with a 0.2 μ m nylon filter, wrapped with aluminum foil and stored at 4°C. To stain calcium deposited, Calcein solution was provided to the cells together with OCM in a proportion of 100:1 (100 μ l of medium + 1 μ l solution Calcein-NaOH).

Remark: *starting from this point, it is important to work in minimal light conditions in order to avoid photobleaching in the sample.*

Unlike Calcein, which stains calcium deposition while the cells are alive, staining with DAPI, Phalloidin and antibodies involves a procedure of two days. Classical fluorescent staining of biological samples takes less time. In this case, stains need to diffuse in a 3D matrix with high collagen concentration, so it takes longer times to reach the target compounds. The protocol for staining the samples is detailed in the following paragraphs.

Day 1: The devices were taken out of the incubator and their OCM was removed by aspirating gently with a pipette. Then, they were cleaned with PBS twice for 5 minutes. The next step is to fix the sample by using paraformaldehyde (PFA). In order to do that, 200 μ l of PFA in a solution of 4% in PBS (Affymetrix) were poured in each device and left for 30 minutes. This step should be done inside a fume hood due to the toxicity of the PFA.

While PAF was fixing living tissue, two solutions for the following steps were prepared:

- 0.1% Triton X-100 solution in PBS (Calbiochem). 1 μ l of Triton X-100 was diluted in 1 ml of PBS. Triton solution is commonly used to permeabilize cell membrane and allow the fluorescent reagents to get the cell body and stain the target compounds.
- 5% Bovine Serum Albumin (BSA, VWR): solution of 5 w/v in PBS which corresponds to 12.5 mg in 250 μ l (each device). This solution was filtered by using a 0.2 μ m filter. BSA solution is a widely used blocking agent that prevents non specific bindings of the fluorescent stains.

After the 30 minutes, PFA was removed with a pipette. Then, the samples were washed three times with PBS. After 3 washing steps, 200 μ l of the solution of Triton X-100 per device were poured. Then, they were left for 30 minutes on a shaker to enhance the processes of diffusion. After that time, the Triton solution was removed with a pipette. The last step was to pour 200 μ l of the BSA 5% solution in each device. Finally, devices were placed on the shaker at 4°C overnight.

Day 2: A solution of BSA 0.5 % in PBS was prepared by diluting the former 5% BSA solution made in day 1 in a total volume of 200 μl per sample: 20 μl of the solution of 5% BSA in PBS and 180 μl of fresh PBS.

At this point, the primary antibody was supplied to the cells. 10 μl of antibody solution (directly provided in the commercial vial) were diluted in 0,5 ml of 0,5% BSA solution. Then, 200 μl of this solution were poured in each device and they are kept for, at least, 6 hours at 4°C on a shaker.

As two targets are studied (BSP2 and DMP1), two solutions were prepared; each one with the corresponding antibody. This way, there were some samples with stained BSP2 and others with stained DMP1.

After the 6 hours, other three steps of washing with PBS were required. Then, secondary antibody, DAPI and phalloidin were given to the culture. The dyeing solution was made in the 0.5% BSA:

- DAPI (1:50): 8 μl of DAPI were diluted in 400 μl of 0.5% BSA solution.
- Phalloidin (1:10): 40 μl were diluted in the same 400 μl of 0.5% BSA solution.
- Secondary antibody (1:50): 8 μl of antibody solution were diluted in the same 400 μl of 0.5% BSA solution.

200 μl of the dyeing solution were poured in each device. Finally, stained samples were kept on the shaker into the fridge overnight (4°C) wrapped with aluminum foil.

Day 3: In order to get the sample ready to use, the samples were taken out of the fridge and the liquid from the medium channels was gently removed with a pipette. Then, samples were washed again with PBS. At this point, it was possible either to watch the samples in a fluorescence/confocal microscope or store them in PBS at 4°C.

Chapter 3

Results

3.1 Alkaline phosphatase production tests

3.1.1 Collagen hydrogel extraction

Collagen hydrogel was extracted from the devices and DNA content of the embedded cells was measured to normalize ALP activity. The gel extraction protocol (detailed in 2.3.2) became a new and innovative technique to isolate cells from the matrix after the culture. The picture below shows the inside of a microfluidic device with three channels before and after the extraction of the collagen hydrogel.

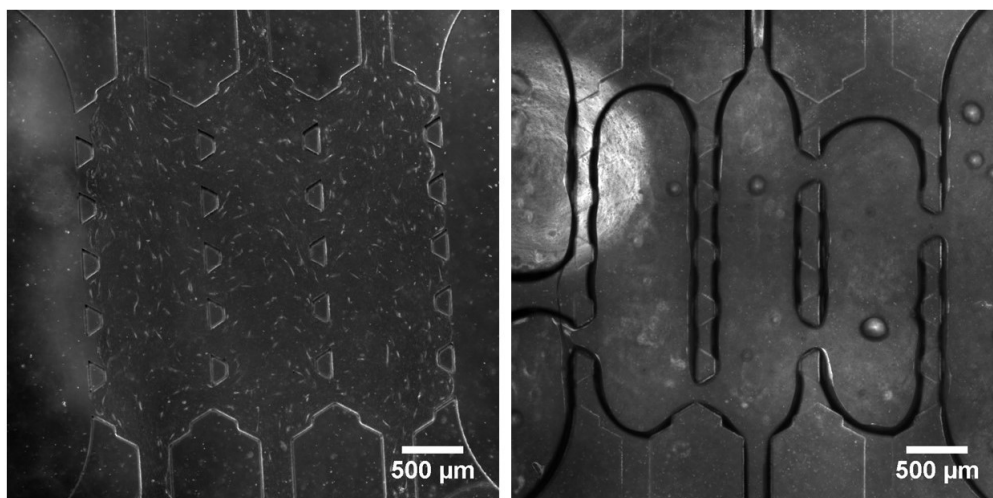


FIGURE 3.1: Brightfield microscope picture (magnified at 2X) of the culture chamber of a microfluidic device before and after the extraction of the gel; left and right respectively. After the extraction, there were not remaining cells inside the chamber but just some rests of PBS around the channels.

3.1.2 ALP activity

It was possible to quantify the ALP activity in the samples following the protocol explained in 2.3.1. The plot below shows the ALP activity before normalizing it (according DNA content) expressed in terms of mili-units (mU) per ml. One unit (U) hydrolyzes 1.0 μmol of pNPP to p-nitrophenol and inorganic phosphate in one hour per minute (at pH 9.8 and at 37°C).

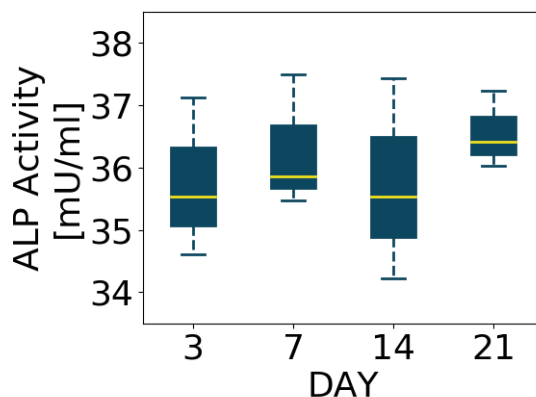


FIGURE 3.2: ALP activity in mU/ml of the HOB at days 3, 7, 14 and 21. Samples were obtained from the 2 hours OCM.

ALP activity was approximately constant over time so there was not a clear decrease in the enzyme activity. Despite that, his value should be normalized to determine if cells were differentiating. In this way, the amount of ALP produced per cell can be calculated.

3.1.3 DNA quantification

The first task was to check the repetitiveness and reliability of both techniques detailed in 2.3.2: Hoechst assay and microvolumes plate. Standards prepared in Hoechst procedure were used to evaluate the outputs of two different techniques.

Standards with lower amount of DNA did not show presence of DNA with both techniques, while comparable values of DNA were observed for standards with higher DNA content. This fact was associated to the standard solution preparation process, due to the small volume of DNA solution added (order of $1\mu\text{l}$). This technical problem made microvolume plate technique more reliable, because it does not need the use of any standard to quantify the DNA concentration in our solution.

Figure 3.3 shows the amount of DNA in the tested samples. Looking at these values, DNA content did not increase significantly over time. Thus, assuming that every microdevice contained approximately the same amount of cells in the beginning, it could be assured that cells did not proliferate in the gel.

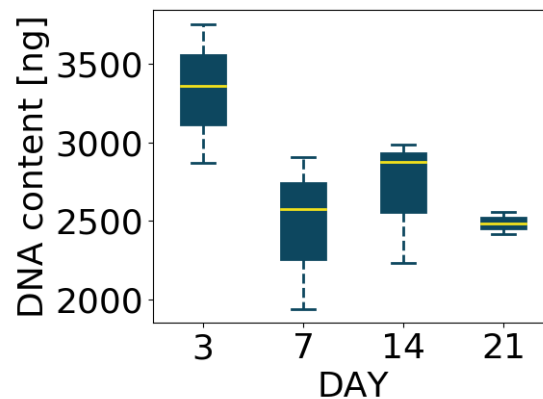


FIGURE 3.3: DNA content in ng of the microfluidic devices at days 3, 7, 14 and 21. The samples were obtained out of the extracted hydrogel and measured with the microvolumes plate.

Values in units of ng DNA/ μ l were provided by the microvolumes plate TAKE3 software. Multiplying this amount by the volume of DNA solution, gives the DNA amount in each sample (figure 3.3). The volume of solution in each sample was not the same because of the variability of the supernatant removed after centrifugation. Volumes of DNA solution in the samples were measured by pipetting.

The highest value of DNA content was seen in the first timepoint. Then, there was a decrease in the genetic material content that kept roughly constant. Assuming that every device contained the same number of cells in the beginning, it can be confirmed that there was not osteoblasts proliferation.

3.1.4 ALP normalization

Normalized ALP activity was obtained by the ratio of the results of the two previous sections (figure 3.4).

The lowest value of ALP activity was present in the first timepoint. Then, at day 7 there was an increase of 24%. After this, normalized ALP activity seemed to have a decreasing trend (approximately 6% from day 7 to day 21). Watching this tendency, it is expected that, the decrease is more pronounced if setting longer timepoints.

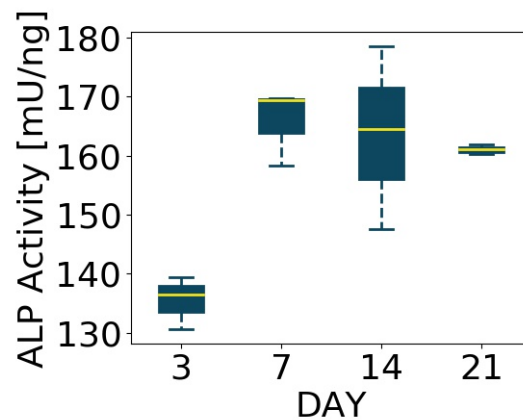


FIGURE 3.4: Normalized ALP activity boxplot according DNA content in the samples at days 3, 7, 14 and 21.

The reduction showed in the plot showed in figure 3.4 was not statistically meaningful. Thus, osteogenic differentiation was not arising after 21 days of culture, seeding 250.000 cells/ml inside the chamber.

3.2 Cell dendrite tracking

One of the main results immediately observed during culture was the difference in cell shapes if they were adhering to the bottom of the device (2D culture) or if they were in the middle of the gel (3D culture). As it can be observed in the figure 3.5, when cells are lied down on the glass (left), they are bigger than those cultured inside the matrix in 3D (right). Moreover, their dendrites are more numerous and longer. These differences can be explained by the cellular mechanobiology and the principles of cell migration in two and three dimensions [48].

Each time of tracking, more dendritic cells were found. This means that cell dendrites number increased with time (figure 3.6). Besides, it can be asserted that dendrites get longer, while cell body gets smaller. This tendency matched with the expected behaviour explained in the introduction chapter.

Apart from the presence of dendrites, several cell-cell connections were tracked and found, emerging in the longest timepoints (figure 3.7). However, those were not comparable to the ones observed in a osteocytic network.

Results obtaining in DNA quantification were double checked in cell tracking: there was not a clear increase in cell content along time (figure 3.8). This fact means that there was not cell proliferation. Providing that, cell number at day 21 was similar to cell number in the beginning of the test.

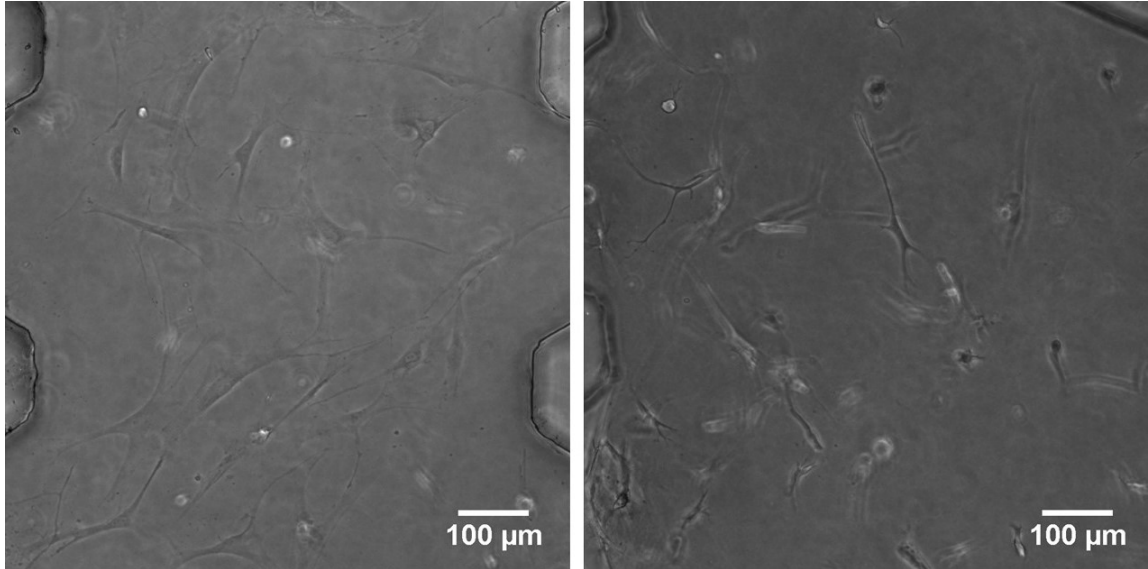


FIGURE 3.5: Brightfield microscope pictures magnified at 10X of 2D cells and 3D cells (left and right respectively) inside a microfluidic device after 21 days of culture.

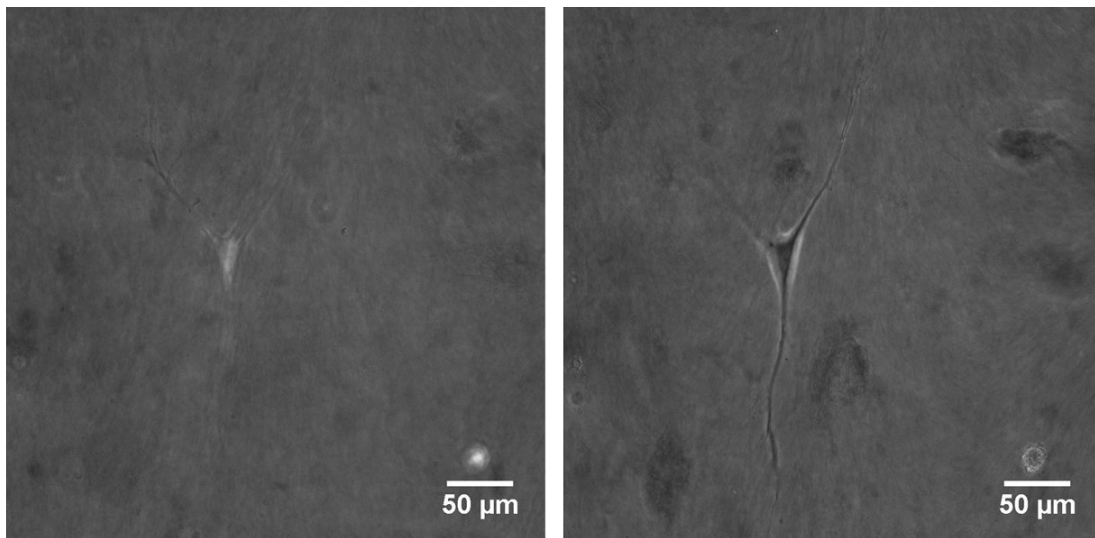


FIGURE 3.6: Two slides of a brightfield microscope *Z-Stack* of a mature and dendritic osteoblast, magnified at 20X

Brightfield microscope pictures can be processed in a software developed in the research group created by *Python: ImagePy*. Over this work, *ImagePy* was utilized in user mode to support dendrite tracking.

The program allows the user to select a region to study and to highlight the dendrites (figure 3.9). Up to now, cell contour is defined manually. However, in a future, cell contour detection will be automatic.

Then, the program is able to distinguish the cell body and the dendrites. It also calculates the length of the dendrites, counts the number of them and the possible connections between cells thanks to powerful image processing tools (figure 3.10).

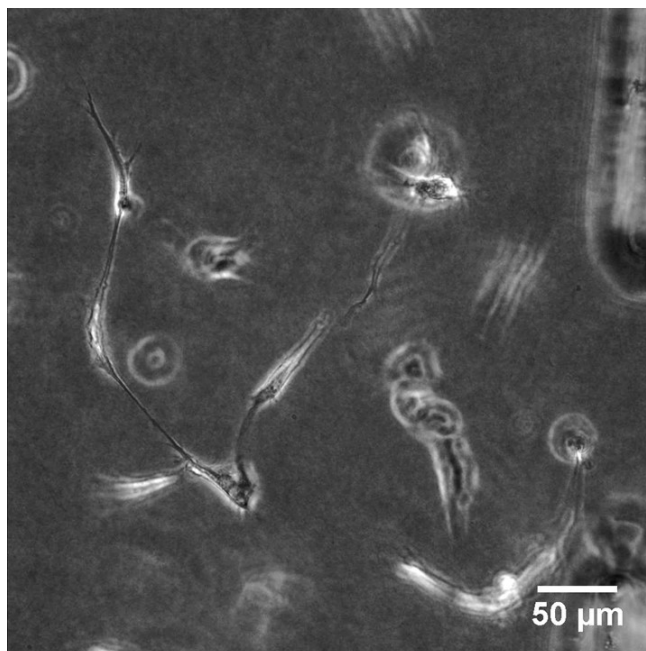


FIGURE 3.7: Brightfield microscope images of cells connection magnified at 20X

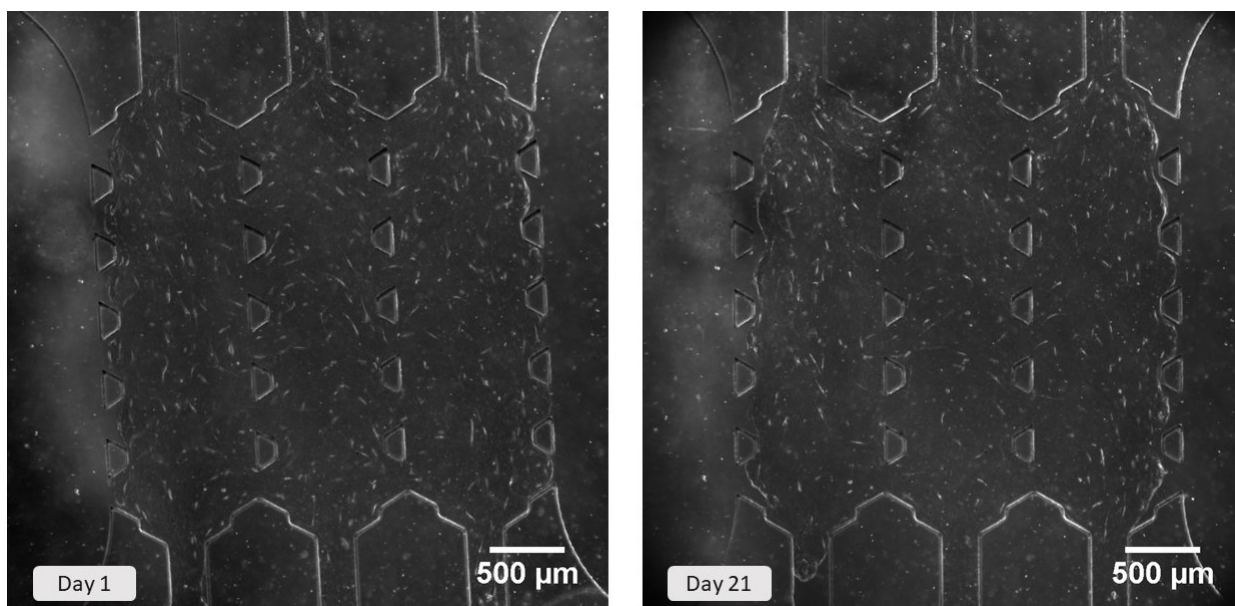


FIGURE 3.8: Brightfield microscope pictures magnified at 2X of the culture chamber at days 1 (left) and 21 (right) of culture

3.3 Osteoblasts mineralization and differentiation

Osteoblasts mineralization was assessed by calcium deposition in the matrix and the expression of protein BSP2. On the other side, osteogenic differentiation would result in expression of protein DMP1. Proteins mentioned above were tracked with proper antibodies and observed in a confocal microscope thanks to the staining detailed in section 2.5.

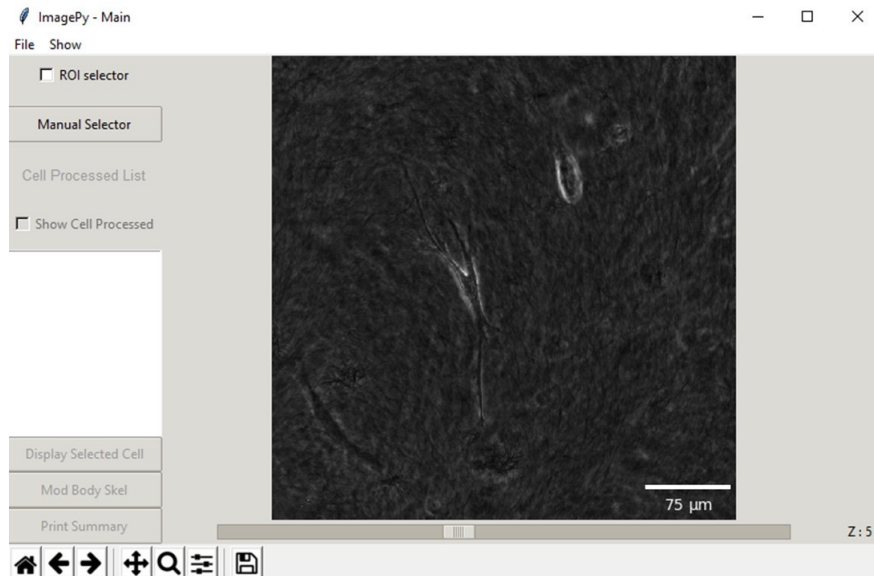


FIGURE 3.9: Interface of the program developed by Python (*ImagePy*). The software is able to open pictures and *Z-stack* in a microscope format and manually select the cell to study

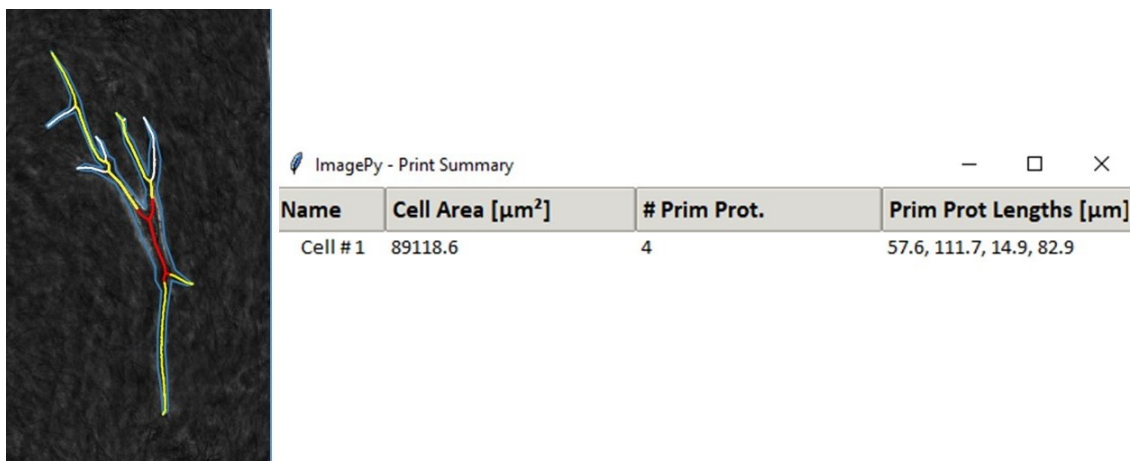


FIGURE 3.10: Analyzed cell by the software *ImagePy*. It is possible to distinguish the cell contour (blue), cell body (red), primary dendrites (yellow) and secondary dendrites (white). The program offers a summary of the cell information (right)

Four samples were used to stain cells and proteins. The samples were incubated up to 28 days, they were stained with Calcein for five days and, finally, fixed. Then, two of them were stained with anti-BSP2 and the other two with anti-DMP1. Finally, every sample got DAPI to bind the cell nuclei.

Figure 3.11 was taken from a sample stained with anti-BSP2, Calcein and DAPI after 28 days of culture. It shows an osteoblast in a mature differentiation phase, which has a considerable amount of calcium released into the matrix, as well as a high expression of BSP2.

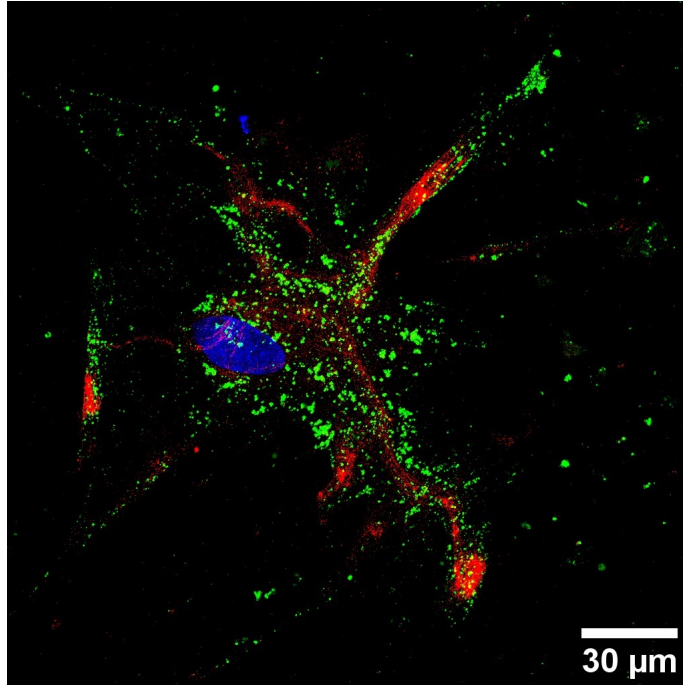


FIGURE 3.11: Confocal microscopy picture of a tridimensional osteoblast magnified at 40X. Cell nuclei has been stained with DAPI (blue), calcium deposition of the matrix and cytoplasm is stained by Calcein (green) and BSP2 protein is stained by immunostaining with an *AlexaFluor* reagent (red)

In contrast, DMP1 staining did not show a significant amount of this protein. Figure 3.12 was taken from a sample stained with anti-DMP1, Calcein and DAPI after 28 days of culture.

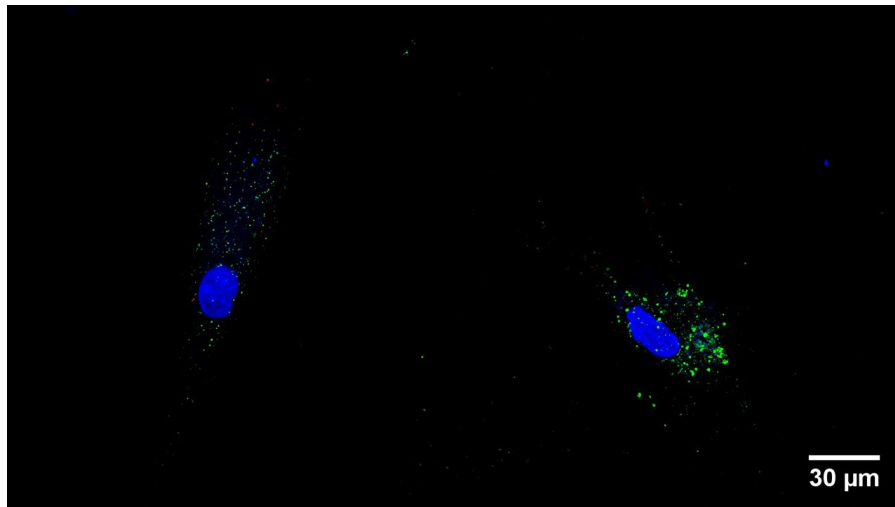


FIGURE 3.12: Confocal microscopy pictures of two tridimensional osteoblasts magnified at 40X. Cell nuclei has been stained with DAPI (blue), calcium deposition of the matrix and cytoplasm is stained by Calcein (green) and DMP1 protein is stained by immunostaining with an *AlexaFluor* reagent (red)

Chapter 4

Discussion

The main goal of this work was to study the feasibility of creating *in vitro* bone models in the microfluidic devices. Apart from that, this work also aimed to achieve long-term culture of bone cells all over the 3D culture environment. In all these experiments, culture conditions were used to induce matrix mineralization and osteogenic differentiation, with a final target to develop a fully differentiated osteocytic phenotype.

Techniques used here demonstrated the possibility of using microfluidics and collagen hydrogel matrix to recreate a tridimensional bone model *in vitro* after culturing primary human osteoblasts for 21 days. Thus, the two first targets of the work were achieved.

Osteoblasts mineralization and differentiation processes were studied by quantifying ALP enzyme activity, tracking calcium deposition and monitoring specific proteins release.

There was not a clear decrease in the ALP activity over time, contrary to what was expected. Nevertheless, Calcium deposition was observed. Regarding these results, some conclusion can be observed: firstly, as there was not a significant reduction of ALP activity over time, osteogenic differentiation was not taking place. Secondly, despite this first result, osteogenic behaviour was achieved because of the presence of the enzyme. Besides, Calcium deposition suggests that osteoblasts mineralization was arising; which also supports the latest assertion.

Those statement were corroborated by the proteins expression tracking. The presence of BSP2 in the matrix confirmed that HOB showed osteogenic behaviour after the culture. On the other side, the absence of DMP1 expression supported the lack of osteocytic differentiation.

ALP quantification protocol succeeded in the correct measurement of the enzyme but there were complications when normalizing activity. The comparison of the two explained techniques to quantify DNA was not possible. Owing to the limited amount of DNA, making triplicates for the Hoechst assay would have led to an excessive dilution of the DNA, confirming that the microvolume plate was the best technique to measure DNA in this case. To solve this trouble, new standard of higher values can be set.

The deficient proliferation of the osteoblasts in the 3D culture involved an underpopulation in the chamber after seeding a density of 250.000 cells/ml. These results and some differences between this work and others on literature suggest that the low cell concentration inside the device limited osteocytic cell transition [13, 20]. This fact means that, the formation of an osteocytic network could be achieved by increasing the cell density in the hydrogel. In this way, the culture could behave similar to bone tissue.

However, a great number of cells in the chamber might compromise the stability of the gel over time. In the figure 3.8-right it can be appreciated a detachment of the gel in the upper corners of the culture chamber. The detachment was caused by the strength of primary osteoblasts when they were migrating. Increasing cell population, this effect is enhanced, so the gel could detach in earlier timepoints. If this problem arises in future tasks, there would be suitable solutions to test. The fastest solution would be to use the protein transglutaminase to fabricate the gel, doing it more resistant to contraction. The second solution, more time consuming but more realistic, would be to seed a high population just in the centre channel of the chamber and, the other two channels would be filled with no-cells hydrogel. In this way, the strength of the culture would not be enough to detach the gel from the posts.

Microfluidic devices demonstrated that they are a powerful tool to study osteoblasts behaviour. Despite many authors have used microfluidics platforms before to study bone cells behaviour [11], this work has been able to create a new 3D bone model *in vitro*. The procedures that have been explained in this document, proved themselves to be a robust tool to assess cell population behavior inside the microdevices in *in vitro* experiments.

However, the expected results were not totally achieved. Some of the limitations of the techniques developed in this work are:

- DNA isolation procedure must be optimized yet. The parameters for centrifuging were modified from the original protocol.
- New control standards should be defined to double check the reliability of microvolume plate. Provided Hoechst assay cannot be performed with the available

equipment, other techniques are suggested on literature, for instance: PicoGreen DNA kit [37].

- The cell density used (250.000 cells/ml) was chosen after some results observed in literature [20]. However, this optimized population did not seem to be enough for the purposes of this work. Mullen *et al* studied mouse bone cell line (MC3T3); which are genetically modified to proliferate more. At the end of their study, the number of present cells were significantly higher [20]. Nevertheless, primary human osteoblasts do not proliferate in 3D as fast as the MC3T3 do (figure 3.8).
- It was not possible to dye cells with both antibodies anti-DMP1 and -BSP2 together with phalloidin due to the proximity of the emission and excitation wavelength between them. Unless phalloidin is used, cell shape cannot be well known. Changing the *Alexa fluor* reagents to immunostain samples, it can be possible to stain a single device to target the two proteins and the cell actin filaments.

Regarding the results obtained in this work, and the limitations mentioned above, next experiments might follow different leads:

- Repeating the experiment with higher cell density and longer timepoints. It is expected that, by increasing the number of cells in the devices, connections arise earlier and in higher numbers. Obtaining this osteocytic network would be the last step of the osteogenic differentiation. This test will be repeated assaying more number of samples in order to run reliable statistics.
- Purchase new primary and secondary antibodies to stain one single device with anti-DMP1 and -BSP2 together with phalloidin. The reagents suggested are the *Alexa fluor 555* and *Alexa fluor 633*.
- As cell might have autofluorescence, negative control microfluidic devices will be imaged to compare emission intensities and delete the background noise from the confocal images.
- Study other markers of osteoblast-osteocyte differentiation. For instance, expression of E11 antigen; a membrane protein more present in transitional cells and in final osteocytes, as well as others extracellular matrix proteins: osteocalcin, osteonectin, fibrinectin, etc [10, 11, 13].

If the desired results are obtained by implementing the new suggestions, many different lines could take advantage of this work. One of the ideas of the long term works is to perform a similar study but seeding cells coming from patients suffering from osteoporosis. By doing this, behaviour of both types would be compared and some conclusions

about the disease could be reached. For instance, it could be possible to find a stimuli to reduce the overcome limitations of osteoporosis.

Another related field of study may involve scaffold-like biomaterials (titanium or degradable polymers) inside the hydrogel. The purpose would be to study the interactions and the cell growth around the biomaterial surface, to get some conclusions about a possible improvement of current bone scaffolds.

Finally, all this result could be extrapolated to the macro-scale, which involves the use of a tool that provides the macro-culture with physiological conditions: mechanical forces and fluid flow. This machine is called bioreactor and it is also a trend field of research in biomedical engineering. In this way, *in vitro* studies on the real scale bone scaffold could be performed.

Most of the recent knowledge on the phenotype and functions of bone cells has been obtained using mouse cells [7, 8, 13, 20, 36, 49, 50]. Mouse cell lines (for instance, MC3T3) are genetically modified bone cells whose behaviour includes a excessive proliferation. They get expressed the same gene of cancer cells, so their original phenotype is inexorably compromised.

Even though the use of mouse cells is widely extended, conclusions cannot be totally extended to human cells. Studies in human cells are limited by their price. However, they can be affordable by using microfluidics.

While most of *in vitro* bone models are developed in 2D, the culture done here is tridimensional. Microfluidic platforms showed in this work provides a tool for performing 3D cultures of human cells in a highly tunable environment

Chapter 5

Conclusions

ALP test was selected from the literature [13, 20] due to its role in osteoblasts activity. The procedure followed was adapted from the literature regarding the available equipment on the M2BE laboratory. The protocol presented in this work succeeded in measuring the ALP activity.

DNA content of the samples could not be measured by using the Hoechst 33258 dye assay. Although this technique was selected from the literature because it is widely used, several problems arose regarding the standard curve to determine the DNA content. Thus, the amount of DNA was measured thanks to a different tool to quantify nuclei acid called as Microvolumes plate.

ALP test demonstrated that osteogenic behaviour was expressed in osteoblasts when they are seeded in the tested conditions. The expression of a mature osteoblastic phenotype was supported by the presence of BMP2 protein. However, the lack of a reduction in ALP activity over time, suggested that no osteoblast-osteocyte differentiation occurred. This issue was also suggested by the lack of DMP1 protein expression in the matrix.

Regarding cell shape, it was achieved a osteocyte shape after some days of culture. Dendrites joined to each other and cells tended to reshape and become a net-shaped structure. However, as there was not cell proliferation, the population inside the hydrogel was lower than expected. Thus, these groups of connected cells were composed of 2, 3 or, maximum, 4 cells.

These techniques are potential methods for reproducing bone tissue-like *in vitro* models. Cells were cultured in a 3D matrix and they end up connected to each other after a long-term culture. Besides, after providing them with the adequate culture conditions, Calcium deposition proved that matrix gets mineralized and the culture showed osteogenic behaviour.

However, a full osteogenic differentiation was not achieved. The negative results obtained here, suggest that a possible solution to get the total osteoblast-osteocyte differentiation is to seed devices with higher cell density and, if possible, extend the timepoints of the experiments.

Appendix A

List of chemicals

Table A.1 shows a list of all chemical reagents used along this work; together with the supplier company and the catalog number of the product.

Compound	Supplier	Catalog number
10X DPBS	Sigma-Aldrich	D1408-500ML
β -Glycerol phosphatase	Sigma-Aldrich	50020-100G
ALP solution	Sigma-Aldrich	P6774-1KU
Ascorbic acid	Sigma-Aldrich	A8960-5G
BSA	VWR	97061-416
Calcein	Sigma-Aldrich	C0875-5G
Collagen Type I, Rat Tail	Corning	354249
Collagenase powder	Sigma-Aldrich	C0130-100MG
DAPI	Invitrogen	D1306
DNA standard	Sigma-Aldrich	D3664-5X1MG
DMEM (low glucose)	Invitrogen	31885-023
EDTA	Sigma-Aldrich	EDS-500G
FBS	Lonza	14-471 F
Glutamine (L-Glutamine)	Lonza	17-605E
Hoechst 33258 dye solution	Sigma-Aldrich	94403-1ML
Human osteoblasts (primary HOB)	PromoCell	C-12720
Mouse IgG secondary 594 nm	Santa Cruz	SC-516178
Mouse IgG secondary 680 nm	Santa Cruz	SC-516180
Mouse monoclonal anti BSP11	Santa Cruz	SC-73630
Mouse monoclonal anti DMPI	Santa Cruz	SC-73633
PBS	Lonza	BE17-516F
PDL	Sigma-Aldrich	P7886-100MG
Penicillin-Streptomycin-Amphotericin B	Lonza	17-745 E
PFA (solution 4% in PBS)	Affimetrix	19943
Phalloidin	Sigma-Aldrich	P1951-.1MG
SIGMAFAST pNPP kit	Sigma-Aldrich	N1891-5SET
Sodium Chloride (NaCl)	Sigma-Aldrich	S5886-1KG
Sodium hydroxide (NaOH)	Sigma-Aldrich	655104-500G
Sylgard 184 (PDMS)	VWR	634165S
TBS	Sigma-Aldrich	T5912-1L
Trypsin (TrypLE&trade)	Invitrogen	12605010
Triton X-100	Calbiochem	648466

TABLE A.1: List of chemical reagents, suppliers and catalog numbers

Bibliography

- [1] D. B. Burr, A. G. Robling, and C. H. Turner. Effects of biomechanical stress on bones in animals. *Bone*, 30(5):781–786, 2002.
- [2] E. H. Burger and J. Klein-Nulend. Mechanotransduction in bone - role of the lacuno-canalicular network. *The FASEB Journal*, 13(9001):S101–S112, 1999.
- [3] N. Kohli, S. Ho, S. J. Brown, P. Sawadkar, V. Sharma, M. Snow, and E. García-Gareta. Bone remodelling in vitro: Where are we headed?: -A review on the current understanding of physiological bone remodelling and inflammation and the strategies for testing biomaterials in vitro. *Bone*, 110:38–46, 2018.
- [4] Z. Deng, Z. Wang, J. Jin, Y. Wang, N. Bao, Q. Gao, and J. Zhao. SIRT1 protects osteoblasts against particle-induced inflammatory responses and apoptosis in aseptic prosthesis loosening. *Acta Biomaterialia*, 49:541–554, 2017.
- [5] M. M. Stevens and J. H. George. Exploring and engineering the cell surface interface. *Science*, 310(5751):1135–1138, 2005.
- [6] A. Piroso, R. Gottardi, P. G. Alexander, and R. S. Tuan. Engineering in-vitro stem cell-based vascularized bone models for drug screening and predictive toxicology. *Stem Cell Research and Therapy*, 9(1), 2018.
- [7] E. Birmingham, G. L. Niebur, P. E. Mchugh, G. Shaw, F. P. Barry, L. M. Mcnamara, and N. Dame. Osteogenic Differentiation of Mesenchymal Stem Cells Is Regulated By Osteocyte and Osteoblast Cells in. 23(353):13–27, 2012.
- [8] M. B. Schaffler, W. Yee Cheung, R. Majeska, and O. Kennedy. Osteocytes: Master orchestrators of bone. *Calcified Tissue International*, 94(1):5–24, 2014.
- [9] R. Florencio-Silva, G. R. D. S. Sasso, E. Sasso-Cerri, M. J. Simões, and P S. Cerri. Biology of Bone Tissue: Structure, Function, and Factors That Influence Bone Cells. *BioMed Research International*, 2015, 2015.
- [10] S. L. Dallas and L. F. Bonewald. Dynamics of the transition from osteoblast to osteocyte. *Annals of the New York Academy of Sciences*, 1192(816):437–443, 2010.

- [11] T. A. Franz-Odenaal, B. K. Hall, and P. E. Witten. Buried alive: How osteoblasts become osteocytes. *Developmental Dynamics*, 235(1):176–190, 2006.
- [12] K. Uchihashi, S. Aoki, A. Matsunobu, and S. Toda. Osteoblast migration into type I collagen gel and differentiation to osteocyte-like cells within a self-produced mineralized matrix: A novel system for analyzing differentiation from osteoblast to osteocyte. *Bone*, 52(1):102–110, 2013.
- [13] M. J. McGarrigle, C. A. Mullen, M. G. Haugh, M. C. Voisin, and L. M. McNamara. Osteocyte differentiation and the formation of an interconnected cellular network in vitro. *European Cells and Materials*, 31(353):323–340, 2016.
- [14] M. Robin, C. Almeida, T. Azais, B. Haye, C. Illoul, J. Lesieur, M. M. Giraud-Guille, N. Nassif, and C. H elary. Involvement of 3D osteoblast migration and bone apatite during in vitro early osteocytogenesis. *Bone*, 88:146–156, 2016.
- [15] L. F. Bonewald and M. L. Johnson. Osteocytes, mechanosensing and Wnt signaling. *Bone*, 42(4):606–615, 2008.
- [16] L. You, S. Temiyasathit, P. Lee, C. H. Kim, P. Tummala, W. Yao, W. Kingery, A. M. Malone, R. Y. Kwon, and C. R. Jacobs. Osteocytes as mechanosensors in the inhibition of bone resorption due to mechanical loading. *Bone*, 42(1):172–179, 2008.
- [17] M. L. Knothe Tate, P. Niederer, and U. Knothe. In vivo tracer transport through the lacunocanalicular system of rat bone in an environment devoid of mechanical loading. *Bone*, 22(2):107–117, 1998.
- [18] C. Palumbo. A three-dimensional ultrastructural study of osteoid-osteocytes in the tibia of chick embryos. *Cell and Tissue Research*, 246(1):125–131, 1986.
- [19] C. Palumbo, M. Ferretti, and G. Marotti. Osteocyte Dendrogenesis in Static and Dynamic Bone Formation: An Ultrastructural Study. *Anatomical Record - Part A Discoveries in Molecular, Cellular, and Evolutionary Biology*, 278(1):474–480, 2004.
- [20] C. A. Mullen, M. G. Haugh, M. B. Schaffler, R. J. Majeska, and L. M. McNamara. Osteocyte differentiation is regulated by extracellular matrix stiffness and intercellular separation. *Journal of the Mechanical Behavior of Biomedical Materials*, 28:183–194, 2013.
- [21] K. Zhang, C. Barragan-Adjemian, L. Ye, S. Kotha, M. Dallas, Y. Lu, S. Zhao, M. Harris, S. E. Harris, J. Q. Feng, and L. F. Bonewald. E11/gp38 Selective

- Expression in Osteocytes: Regulation by Mechanical Strain and Role in Dendrite Elongation. *Molecular and Cellular Biology*, 26(12):4539–4552, 2006.
- [22] E. L. George, S. L. Truesdell, Spencer L. York, and M. M. Saunders. Lab-on-a-chip platforms for quantification of multicellular interactions in bone remodeling. *Experimental Cell Research*, 365(1):106–118, 2018.
- [23] P. Abgrall and A. M. Gué. Lab-on-chip technologies: Making a microfluidic network and coupling it into a complete microsystem - A review. *Journal of Micromechanics and Microengineering*, 17(5), 2007.
- [24] G. M. Whitesides. The origins and the future of microfluidics. *Nature*, 442(7101):368–373, 2006.
- [25] O. Moreno-Arotzena, C. Borau, N. Movilla, M. Vicente-Manzanares, and J. M. García-Aznar. Fibroblast Migration in 3D is Controlled by Haptotaxis in a Non-muscle Myosin II-Dependent Manner. *Annals of Biomedical Engineering*, 43(12):3025–3039, 2015.
- [26] C. Del Amo, C. Borau, N. Movilla, J. Asín, and J. M. Garcia-Aznar. Quantifying 3d chemotaxis in microfluidic-based chips with step gradients of collagen hydrogel concentrations. *Integrative Biology*, 9(4):339–349, 2017.
- [27] D. Huh, Y. Torisawa, G. A. Hamilton, H. J. Kim, and D. E. Ingber. Microengineered physiological biomimicry: organs-on-chips. *Lab on a Chip*, 12(12):2156–2164, 2012.
- [28] C. Del Amo, V. Olivares, M. Córdor, A. Blanco, J. Santolaria, J. Asín, C. Borau, and J. M. García-Aznar. Matrix architecture plays a pivotal role in 3d osteoblast migration: The effect of interstitial fluid flow. *Journal of the mechanical behavior of biomedical materials*, 83:52–62, 2018.
- [29] Y. Shin, S. Han, J. S. Jeon, K. Yamamoto, I. K Zervantonakis, R. Sudo, R. D. Kamm, and S. Chung. Microfluidic assay for simultaneous culture of multiple cell types on surfaces or within hydrogels. *Nature Protocols*, 7:1247, jun 2012.
- [30] P. G. Buxton, M. Bitar, K. Gellynck, M. Parkar, R. A. Brown, A. M. Young, J. C. Knowles, and S. N. Nazhat. Dense collagen matrix accelerates osteogenic differentiation and rescues the apoptotic response to MMP inhibition. *Bone*, 43(2):377–385, 2008.
- [31] C. Valero, H. Amaveda, M. Mora, and J. M. García-Aznar. Combined experimental and computational characterization of crosslinked collagen-based hydrogels. *PLoS ONE*, 13(4):1–16, 2018.

- [32] M. M. Giraud Guille, C. Helary, S. Vigier, and N. Nassif. Dense fibrillar collagen matrices for tissue repair. *Soft Matter*, 6(20):4963–4967, 2010.
- [33] E. Birmingham, G. L. Niebur, and P. E. McHugh. Osteogenic differentiation of mesenchymal stem cells is regulated by osteocyte and osteoblast cells in a simplified bone niche. *European Cells and Materials*, 23:13–27, 2012.
- [34] P.-H. Wu, A. Giri, S. X. Sun, and D. Wirtz. Three-dimensional cell migration does not follow a random walk. *Proceedings of the National Academy of Sciences*, 111(11):3949–3954, 2014.
- [35] D. Turhani, B. Cvikl, E. Watzinger, M. Weißenböck, K. Yerit, D. Thurnher, and R. Lauer, G. and Ewers. In vitro growth and differentiation of osteoblast-like cells on hydroxyapatite ceramic granule calcified from red algae. *Journal of Oral and Maxillofacial Surgery*, 63(6):793–799, 2005.
- [36] E. Leclerc, B. David, L. Griscom, B. Lepioufle, T. Fujii, P. Layrolle, and C. Legalaisa. Study of osteoblastic cells in a microfluidic environment. *Biomaterials*, 27(4):586–595, 2006.
- [37] Y. Sai, Y. Shiwaku, T. Anada, K. Tsuchiya, T. Takahashi, and O. Suzuki. Capacity of octacalcium phosphate to promote osteoblastic differentiation toward osteocytes in vitro. *Acta Biomaterialia*, 69:362–371, 2018.
- [38] P. Bianco, M. Riminucci, E. Bonucci, J. D. Termine, and P. G. Robey. Bone sialoprotein (BSP) secretion and osteoblast differentiation: Relationship to bromodeoxyuridine incorporation, alkaline phosphatase, and matrix deposition. *Journal of Histochemistry and Cytochemistry*, 41(2):183–191, 1993.
- [39] G. J. Atkins, D. M. Findlay, P. H. Anderson, and H. A. Morris. *Target genes: Bone proteins*, volume 25. Elsevier, third edition edition, 2011.
- [40] Y. Mikuni-Takagaki, Y. Kakai, M. Satoyoshi, E. Kawano, Y. Suzuki, T. Kawase, and S. Saito. Matrix mineralization and the differentiation of osteocyte-like cells in culture. *Journal of Bone and Mineral Research*, 10(2):231–242, 1995.
- [41] Y. Nakano, W. Beertsen, T. Vandenbos, T. Kawamoto, K. Oda, and Y. Takano. Site-specific localization of two distinct phosphatases along the osteoblast plasma membrane: Tissue non-specific alkaline phosphatase and plasma membrane calcium ATPase. *Bone*, 35(5):1077–1085, 2004.
- [42] J. Q. Feng, H. Huang, Y. Lu, L. Ye, Y. Xie, T. W. Tsutsui, T. Kunieda, T. Castriano, G. Scott, and L. B. Bonewald. The dentin matrix protein 1 (dmp1) is specifically expressed in mineralized, but not soft, tissues during development. *Journal of dental research*, 82(10):776–780, 2003.

- [43] C. Del Amo, C. Borau, N. Movilla, J. Asín, and J. M. García-Aznar. Quantifying 3D chemotaxis in microfluidic-based chips with step gradients of collagen hydrogel concentrations. *Integrative Biology (United Kingdom)*, 9(4):339–349, 2017.
- [44] Population Cytogenetics Unit and Western General. Collagen studies substrata for Cell Cultures Collection and Solubilization Procedures for Counting Petri Dish Cultures Labeled Preparation of Hydrated Collagen Lattices. *The Journal of Cell Biology*, pages 626–637, 1972.
- [45] S. L. Schor. Cell proliferation and migration on collagen substrata in vitro. *Journal of cell science*, 41:159–75, 1980.
- [46] Y. J. Kim, R. L. Y. Sah, J. H. Doong, and A. J. Grodzinsky. Fluorometric assay of DNA in cartilage explants using Hoechst 33258. *Analytical Biochemistry*, 174(1):168–176, 1988.
- [47] Nucleic Acid Quantitation Using BioTek 's Scanning Microplate Spectrophotometer. *BIOTEK, Get better reaction*, (9), 2006.
- [48] C. Decaestecker, O. Debeir, P. Van Ham, and R. Kiss. Can anti-migratory drugs be screened in vitro? A review of 2D and 3D assays for the quantitative analysis of cell migration. *Medicinal Research Reviews*, 27(2):149–176, 2007.
- [49] H. Yamamoto, B. Ramos-Molina, A. N. Lick, M. Prideaux, V. Albornoz, L. Bonewald, and I. Lindberg. Posttranslational processing of FGF23 in osteocytes during the osteoblast to osteocyte transition. *Bone*, 84:120–130, 2016.
- [50] K. Irie, S. Ejiri, Y. Sakakura, T. Shibui, and T. Yajima. Matrix mineralization as a trigger for osteocyte maturation. *Journal of Histochemistry and Cytochemistry*, 56(6):561–567, 2008.